



LOW CARBON LIVING  
CRC

## Field Investigation of Biogenic Corrosion of Mortar Specimens at North Head Wastewater Treatment Plant

Project: RP1020u2



Authors	Hammad Anis Khan, Arnaud Castel, James Aldred, Stephen Foster and Jerry Sunarho
Title	Field Investigation of Biogenic Corrosion of Mortar Specimens at North Head Wastewater Treatment Plant
ISBN	
Date	30/10/2019
Keywords	Geopolymer concrete, Wastewater, Biogenic Corrosion
Publisher	Cooperative Research Centre for Low Carbon Living
Preferred citation	Khan, H.A., Castel, A., Aldred, J., Foster, S.J., and Sunarho, J. (2019). <i>Field Investigation of Biogenic Corrosion of Mortar Specimens at North Head Wastewater Treatment Plant</i> . CRC for Low Carbon Living, Sydney.



Australian Government  
Department of Industry,  
Innovation and Science

**Business**  
Cooperative Research  
Centres Programme

## Acknowledgements

This research was funded by the CRC for Low Carbon Living Ltd supported by the Cooperative Research Centres program, an Australian Government initiative.

The experimental work was carried out in the Materials and Structures Laboratory at the School of Civil and Environmental Engineering, UNSW Sydney, Australia. The project could not have been undertaken without the strong and valued contribution of our many industry partners: Sydney Water, Australasian (iron & steel) Slag Association (ASA) and Ash Development Association of Australia (ADAA). The strong support of each is acknowledged with thanks.

## Disclaimer

Any opinions expressed in this document are those of the authors. They do not purport to reflect the opinions or views of the CRCLCL or its partners, agents or employees.

The CRCLCL gives no warranty or assurance and makes no representation as to the accuracy or reliability of any information or advice contained in this document, or that it is suitable for any intended use. The CRCLCL, its partners, agents and employees, disclaim any and all liability for any errors or omissions or in respect of anything or the consequences of anything done or omitted to be done in reliance upon the whole or any part of this document.

## Peer Review Statement

The CRCLCL recognises the value of knowledge exchange and the importance of objective peer review. It is committed to encouraging and supporting its research teams in this regard.

The author(s) confirm that this document has been reviewed and approved by the project's steering committee and by its program leader. These reviewers evaluated its:

- originality
- methodology
- rigour
- compliance with ethical guidelines
- conclusions against results
- conformity with the principles of the Australian Code for the Responsible Conduct of Research (NHMRC 2007),

and provided constructive feedback which was considered and addressed by the author(s).

## Table of Contents

Executive Summary .....	5
1 Introduction .....	6
2 Research Significance .....	6
3 Specimen Preparation.....	6
3.1 Materials .....	7
3.2 Mix proportions .....	8
3.3 Mixing and curing .....	9
3.4 Initial observations.....	9
4 Experimental Program .....	10
4.1 Fabrication of assembly and placement of specimen .....	10
4.2 Site location .....	11
4.3 Atmospheric condition assessment.....	11
4.4 Placement of specimens in digester.....	11
4.5 Characterization of the environmental conditions .....	14
4.6 Specimen collection and analyses performed.....	14
5 Experimental Results .....	14
5.1 Visual observations .....	16
5.2 Variation in mass and compressive strength .....	19
5.3 Porosity and dry bulk density .....	19
5.4 Reduction in surface pH .....	22
5.5 Depth of neutralization and pH profile .....	22
5.6 X-Ray diffraction analysis .....	30
5.7 Scanning electron microscopy with EDX analysis .....	34
6 Conclusions .....	38
References .....	

## List of Tables

Table 1. Chemical Composition of FA, Slag, SR cement, CAC and MM using XRF analysis. ....	7
Table 2. Mix Proportion of FA-GPm, AASm, SRPCm and CACm. ....	8
Table 3. Physical properties and observations. ....	9
Table 4. Tag colour coding. ....	11
Table 5a. Visual observations after 6, 12, 24 and 36 months of exposure: FA-GPm specimens. ....	16
Table 6. Compressive strength loss at 24 and 36 months. ....	21
Table 7. Porosity and dry bulk density changes at 24 and 36 months. ....	21
Table 8. Average depth of neutralisation after exposure to on-site conditions. ....	27
Table 9. Average depth of deterioration after 36 months of exposure to on-site conditions. ....	36

## List of Figures

Figure 1. Stages of corrosion in new concrete with hypothesized microorganism's succession during MICC proposed by Islander et al. [14]. ....	7
Figure 2. Specimen to be sealed for exposure condition. ....	10
Figure 3. Net assembly for hanging specimens: dimensions (left) and after construction (right). ....	10
Figure 4. Specimen with the net assembly ready to be placed on site. ....	11
Figure 5. Aerial view of North Head Wastewater Treatment Plant showing digesters 1 to 3. ....	12
Figure 6. Digesters at site for hanging the specimens. ....	12
Figure 7. Left: Odalog data logger placed inside the drain for measuring H <sub>2</sub> S concentration and temperature. Right: Specimens placed inside of drain. ....	12
Figure 8. Specimen's hanging pattern in each Digesters. ....	13
Figure 9. Environmental conditions in each digester. ....	15
Figure 10. Variation in mass observed during 36 months of exposure. ....	20
Figure 11. Variation in surface pH observed during 36 months of exposure: specimens from (a) digester 1, (b) digester 2 and (c) digester 3. ....	23
Figure 12. Neutralization depth indicated by phenolphthalein. ....	24
Figure 13. pH profile of specimens with respect to exposure duration and location. ....	28
Figure 14. XRD pattern of FA-GPm after 36 months of exposure in digester 1. ....	31
Figure 15. XRD pattern of AASm after 36 months of exposure in digester 1. ....	31
Figure 16. XRD pattern of CACm after 36 months of exposure in digester 1. ....	33
Figure 17. XRD pattern of MM after 36 months of exposure in digester 1. ....	33
Figure 18. XRD pattern of SRPCm after 36 months of exposure in digester 1. ....	34
Figure 19. SEM images of deteriorated region within FA-GPm, AASm, CACm, MM and SRPCm after 36 months of exposure in each digester. ....	35
Figure 20. Sulphur mapping of deteriorated region within FA-GPm, AASm, CACm, MM and SRPCm after 36 months of exposure in each digester with. ....	37

## Executive Summary

This report outlines the results of a three-year study into biogenic corrosion of mortar in an aggressive environment. While concrete is one of the most widely used materials in the transportation and treatment of sewage, it is subject to rapid decay under in a sewage environment due to acids produced due to the action of bacterial and fungal species combined with sulphate attack. The effect of the biogenic or microbially induced corrosion of concrete in sewers can be many millimetres per year. The rate of corrosive attack on concrete is dependent on the type of cementitious material used, exposure environment and the materials microstructure.

Many researchers have tested the performance of ordinary Portland cement (OPC) and calcium aluminate cement (CAC) concrete against microbially induced attack. While the durability and performance of alkali-activated binder systems of fly ash and slag have been tested for sulphuric acid attack, resistance to microbial induced concrete corrosion needs to be researched. This study subjects five different binder systems to highly aggressive environments within an operating wastewater treatment plant. The results may be used to provide a comparative performance of each of the tested binders and as a guide plant owners, designers and future researchers.

The three-year testing program took place at Sydney Water's North Head Wastewater Treatment Plant (WWTP) in Manly, Sydney, Australia. This is the second largest WWTP servicing Sydney, with a population of 4.6 million – the plant runs 24 hours a day, 7 days a week, 52 weeks of the year. The WWTP maintains three digesters, where the specimens were placed. Specimens were hung in the digesters to study the behaviour of mortars in this ultra-aggressive environment. The atmospheric concentration of hydrogen sulphide ( $H_2S$ ) in the digesters often exceed 500 parts per million (ppm), with daily averages regularly spiking above 150 ppm. Over the three-year period of the study, the average daily  $H_2S$  conditions was 40 ppm in digester 1, 7 ppm in digester 2 and 24 ppm in digester 3. Overall, digester 1 was much more aggressive compared to digesters 2 and 3.

Five mix designs were tested: three trial mixes consisting of a fly ash geopolymer mix (FA-GPm), a slag based geopolymer mix (AASm) and a sulphate resistant Portland cement mix (SRPCm), and two commercial mixes, a calcium aluminate cement and aggregate system (CACm) and a proprietary

slag based geopolymer (MM). The main conclusions drawn are:

- The FA-GPm and CACm specimens remained structurally intact with only minor surface coarsening.
- The AASm and SRPCm specimens showed major deterioration with loss of surface material and crack propagation.
- The MM experienced around 2 mm loss of surface material.
- Deterioration within AASm and SRPCm specimens were pronounced compared to FA-GPm, MM and CACm in terms of mass and strength. The CACm showed gain in mass with time.
- Based on the assessment of visible deterioration, mass loss, strength reduction, porosity and bulk density, CACm showed good performance.
- FA-GPm and AASm specimens show a higher porosity compared to other mixes.
- Surface pH values and estimation of time required to initiate the Stage II microbially induced concrete corrosion was less in FA-GPm compared to other mortars.
- The depth of the reduction in pH was significant in FA-GPm mix.
- The depth of pH reduction was lower in CACm compared to FA-GPm, AASm, MM and SRPCm, indicating resilience towards loss in alkalinity and, hence, protection to any reinforcing steel located near the exposed surface.
- SEM imagery showed the microstructural deterioration, crystallization of gypsum and weakening of interfacial transition zone (ITZ) between aggregate and binder.
- The depth of deterioration in the AASm and SRPCm specimens was greater than for CACm and MM.

The detailed design of the mix is crucial in these very aggressive sewer environments, and care is needed in translating these results to those of similar binder systems. Various combinations of source materials, of activators and the resulting microstructure will likely lead to differing results. While Geopolymer binders show considerable promise, further research is needed in developing, and optimising, these systems.

## 1 Introduction

Concrete is one of the most widely used construction materials in wastewater treatment collection and transportation infrastructure. However, it is susceptible to multistage deterioration in highly acidic environments. This results in the degradation of microstructure and performance failure with the passage of time. The main cause of this degradation is the corrosion of concrete due to the in-situ production of sulfuric acid by bacteria. This mechanism is known as microbially induced or biogenic corrosion of concrete [1].

Microbially induced concrete corrosion (MICC), is a multi-stage process (Figure 1) that can reduce the usable life of the concrete to 30–50 years, and in extreme cases to a few years [2]. The effects of the corrosive attack of concrete in sewers can be of the order of many mm per year, a significant component of this damage caused by sulphuric acid or sulphate attack [3]. Corrosive attack on concrete is very much dependant on the type of cementitious material used, exposure environment and the materials microstructure. The development of an accurate and accelerated test procedure is essential to better comprehend the processes and mechanisms involved in all cementitious material. However, to develop such test some additional knowledge is required. This can be achieved by studying in-situ conditions to determine the biochemical processes and morphological changes taking place in the concrete matrix as a result of bio deterioration.

Geopolymer cement is produced by combining an alkaline solution, such as sodium hydroxide (NaOH), potassium hydroxide (KOH), sodium silicate ( $\text{Na}_2\text{SiO}_3$ ) or potassium silicate ( $\text{K}_2\text{SiO}_3$ ), to activate aluminosilicate materials [4]. These materials commonly include fly ash, metakaolin and ground granulated blast furnace slag (GGBFS). The microstructure of geopolymer is build-up of randomly linked tetrahedrons of negatively charged  $(\text{SiO}_4)^{-4}$  and

$(\text{AlO}_4)^{-5}$  balanced by cation  $\text{M}^+$  ( $\text{Na}^+$  or  $\text{K}^+$ ) making a three-dimensional amorphous network. This network forms a sodium aluminosilicate (N-A-S-H) gel, which has been demonstrated to perform better in acidic environments than conventional ordinary Portland cement (OPC) concrete [5, 6].

## 2 Research Significance

Multiple researches have performed tests on both the performance of OPC binder systems and geopolymer systems in microbially corrosive environments and for resistance to sulphuric acid [1, 2, 7-16] by exposing them to  $\text{H}_2\text{SO}_4$  [5, 17-20]. The durability and performance of alkali-activated binder systems of fly ash and slag, however, in MICC environments needs to be researched and proven. This study subjects five different binder systems to highly aggressive microbial environments within an operating wastewater treatment system, with the results used to provide a comparative performance of each of the tested binder system and guide plant owners and designers.

## 3 Specimen Preparation

Five different mortar specimens were prepared for a field investigation of cubes placed in a corrosive environment at Sydney Water's North Head Wastewater Treatment Plant. The first mix is low calcium fly ash based geopolymer mortar (FA-GPm), the second was an alkali-activated slag-based mortar (AASm) and the third was sulphate resistant ordinary Portland cement-based mortar (SRPCm). All three have the same amount of binder and aggregate. In addition to these three, for comparative study two commercially available mortars were also prepared; namely, a calcium aluminate cement and calcium aluminate aggregate mortar (CACm) and a slag based geopolymer mortar (MM).

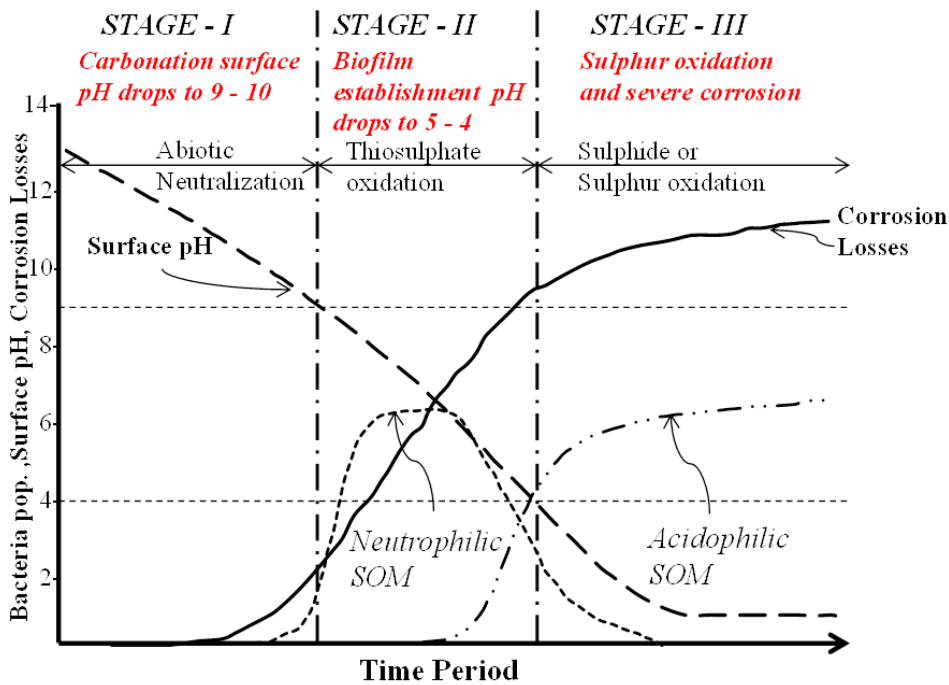


Figure 1. Stages of corrosion in new concrete with hypothesized microorganism's succession during MICC proposed by Islander et al. [14].

### 3.1 Materials

Low calcium type fly ash (ASTM C 618 Class F) has been used to manufacture the FA-GPm. The source of this FA is Eraring power station in New South Wales, Australia. GGBFS was also used as an aluminosilicate source in both FA-GPm and AASm, whereas SR cement (ASTM C 150 Type V) was used to prepare the SRPCm specimens. Table 1 gives the chemical composition of the binders using X-ray fluorescence (XRF) analysis. Sydney sand in a

saturated surface dry (SSD) condition was used as fine aggregate having a specific gravity of 2.65 and water absorption of 3.5%. Tap water was used for mixing. The CAC and MM mortar contain premixed fine aggregate and, thus, do not require the addition of sand. MM is premixed with fine sand which would explain the high silica content.

The CAC mortar has a combination of CA cement with alag (CA aggregate) having aggregate to binder ratio of around 2.0.

Table 1. Chemical Composition of FA, Slag, SR cement, CAC and MM using XRF analysis.

Chemical Oxides	FA (wt. %)	GGBFS (wt. %)	SR Cement (wt. %)	CAC (wt. %)	MM (wt. %)
SiO <sub>2</sub>	66.56	31.52	28.19	6.76	59.49
Al <sub>2</sub> O <sub>3</sub>	22.47	12.22	10.35	42.27	6.38
Fe <sub>2</sub> O <sub>3</sub>	3.54	1.14	1.64	11.05	1.93
CaO	1.64	44.53	51.78	36.42	22.66
MgO	0.65	4.62	3.47	0.7	2.74
Na <sub>2</sub> O	0.58	0.21	0.2	0.21	0.516
K <sub>2</sub> O	1.75	0.33	0.38	0.28	1.1
MnO	0.06	0.36	-	0.13	-
P <sub>2</sub> O <sub>5</sub>	0.11	0.02	-	0.112	0.07
TiO <sub>2</sub>	0.88	1.03	0.71	1.92	0.297
SO <sub>3</sub>	0.1	3.24	2.98	0.07	2.26
Loss on ignition (LOI)	1.66	0.79	0.39	1.34	2.55



### 3.2 Mix proportions

The mix design of FA-GPm is derived from the research performed by Noushini et al. [21] with minor modifications and laboratory trial mixes. All three FA-GPm, AASm and SR cement mortar had the same amount of binder and aggregate. For the geopolymer mortars, aluminosilicate binder (i.e. FA and GGBFS) was used. To activate the binder, an alkaline solution was used having a mixture of sodium hydroxide (NaOH) and sodium silicate ( $\text{Na}_2\text{SiO}_3$ ) solution. The ratio of sodium silicate to sodium hydroxide solution used was set to 2.5:1 (by mass). The NaOH solution was prepared by dissolving sodium hydroxide pellets in water. The concentration of sodium hydroxide solution used was 12 molar (M), which consisted of 480 grams of sodium hydroxide pellets per litre of sodium hydroxide solution or 361 grams of sodium hydroxide pellets per kilogram of sodium hydroxide solution. Sydney tap water was used in this study as the solvent to produce the sodium hydroxide solution.

Both the alkaline activator solutions were prepared and mixed 24 hours prior to use. The mass ratio of alkaline activator to binder in FA-GPm and AASm was selected to be 0.5. The FA-GPm mix consisted of  $615 \text{ kg/m}^3$  of SCM binder, having 85% of FA and 15% of GGBFS; whereas, the AASm mix has  $615 \text{ kg/m}^3$  of SCM binder, with

75% of GGBFS and 25% of FA. The total mass of water in these alkali-activated mixes was estimated as the sum of mass of water in sodium silicate solution and the mass of water added to prepare the sodium hydroxide solution, in addition to free water added while mixing. Similarly, the total binder content of these mixes includes the SCMs (FA and GGBFS), the anhydrous sodium hydroxide flakes and solid part of sodium silicate solution (mass of  $\text{SiO}_2$  and  $\text{Na}_2\text{O}$ ). These two factors are used to calculate the water to binder ratio for FA geopolymer and alkali-activated slag-based mortars. Calcium aluminate cement mortar (CACm) and sulphate resistant Portland cement mortar (SRPCm) mixes were the counterparts of alkali-activated mixes having same amount of binders, i.e.  $615 \text{ kg/m}^3$  and fine aggregate.

Considering that the mortar mixes were to be exposed to aggressive field conditions, the characteristic compressive strength of 40 MPa after 28 days of curing was set. Water to cement ratio was estimated to be 0.42. Table 2 gives the mix proportion of the mortars. The aggregate mass presented in Table 2 is under saturated surface dry (SSD) condition. The technical data sheet of slag based geopolymer mortar suggests that the water/powder ratio must be kept below 0.2. To get the desired workability and strength a water/powder ratio of 0.185 was adopted.

Table 2. Mix Proportion of FA-GPm, AASm, SRPCm and CACm.

Components	FA-GPm ( $\text{kg/m}^3$ )	AASm ( $\text{kg/m}^3$ )	SRPCm ( $\text{kg/m}^3$ )	CACm ( $\text{kg/m}^3$ )
Sydney Sand	1230	1230	1230	-
CA aggregate	-	-	-	1230
FA	522.75	153.75	-	-
GGBFS	92.25	461.25	-	-
SR cement	-	-	615	-
Sodium hydroxide solution (NaOH)	87.87	87.87	-	-
Calcium aluminate cement (CAC)	-	-	-	615
Sodium Silicate solution ( $\text{Na}_2\text{SiO}_3$ )	219.7	219.7	-	-
Free Water	25	25	258	258
Total Binder (cement or SCM)	615	615	615	615
Water/binder (including activator solids)	0.31	0.31	0.42	0.42
Activator/SCM	0.5	0.5	-	-
Sodium Silicate/Sodium hydroxide ( $\text{Na}_2\text{SiO}_3/\text{NaOH}$ )	2.5	2.5	-	-
Molarity of Sodium hydroxide solution	12M	12M	-	-

### 3.3 Mixing and curing

All five types of mortars were mixed in a Hobart mixer using the sequence outlined below. For the case of FA-GPm and AASm, all the SSD condition aggregate and SCM were first dry mixed for five minutes, except for GGBFS in FA-GPm, to achieve uniform dispersion. After that water and activator were gradually added and mixed for a further five minutes. Finally, the slag was introduced in FA-GPm and further mixing was done for five minutes. After scrapping the blades and sides of the mixer, another two minutes of mixing was performed at a medium speed.

For the CACm and SRm mixes, the solid contents, which include all the SSD condition fine aggregates and cement binder, were first dry mixed for five minutes to achieve uniform dispersion. Water was gradually added and mixed for another five minutes. The moulds were cleaned thoroughly and were coated with a thin layer of demoulding grease, to facilitate the demoulding process. For the case of proprietary geopolymer mortar (MM), water was added as instructed in technical datasheet. The freshly mixed mortar was poured into cubical steel moulds, of 50 mm dimension on each side, in two layers. External compaction was applied via a vibrating table to achieve good consolidation.

Three different types of curing techniques were adopted for these mortar specimens; namely, heat curing, water curing and ambient curing. Water curing was applied on SRPCm, whereas ambient curing was used for CACm, AASm and MM mixes.

After demoulding, SRPCm specimens were placed for 2 weeks in lime saturated water for final curing. The other three were placed in an

airtight plastic bag for 7 days, after the specimens were taken out of their bag and placed in the environmental room (at 23°C and 50% relative humidity) until the start of the field placement.

Since strength development and geopolymerization can be slow in low calcium FA based geopolymer mortar; heat curing was employed on FA-GPm to achieve the required strength. The FA-GPm specimens were sealed in plastic bags and stored in an oven at 75°C for 18 hours after casting was finished. Following the heat curing, the FA-GPm specimens were demoulded and stored in an environmental room at a temperature of 23°C and relative humidity (RH) of 50% until the start of the experiments.

After casting the AASm, CACm, SRPCm and MM specimens were covered with a damp cloth and sealed in a plastic bag for 24 hours and kept at 23°C. After 24 hours damp curing in the plastic bag, the specimens were stored in an environmental room at a temperature of 23°C and relative humidity (RH) of 50% until the start of the experiments.

### 3.4 Initial observations

A total of 30 cube specimens for each mix design were prepared for placement on site conditions. Table 3 presents the initial physical properties (compressive strength, surface pH, bulk porosity and dry bulk density) of the various mixes at the time the specimens were placed on site. The surface pH of FA-GPm was 11.4 whereas; SRPCm, MM and AASm had pH values of 12.7, 12.3 and 12.6, respectively. This higher pH is due to the high amount of calcium within the raw materials used (Table 1). The surface pH of CACm was similar to that of FA-GPm.

Table 3. Physical properties and observations.

Properties	FA-GPm	AASm	SRPCm	CACm	MM
Compressive strength (MPa) ± SD					
24 hour	42.3±0.9	41.6±2.5	10.6±1.9	26.5±2.1	18.8±1.1
7 days	44.1±1.8	63.5±1.3	24.3±1.4	52.7±2.3	38.4±1.6
28 days	47.8±1.6	80.4±2.1	50.7±1.7	64.1±1.9	56.3±1.8
Average weight (gms)	254.3±4.7	285.9±3.1	281.4± 5.8	293.4±3.2	277.5±2.9
Porosity (%) ± SD	18.3±0.05	15.8±0.06	17.7±0.11	15.5±0.15	12.3±1.1
Dry Bulk Density (Kg/m <sup>3</sup> ) ± SD	1713±1.0	1935±4.6	1890±0.3	2027±8.2	1991±9.2
Surface pH ± SD	11.4±0.4	12.6±0.36	12.7±0.21	11.5±0.2	12.3±1.0

## 4 Experimental Program

### 4.1 Fabrication of assembly and placement of specimen

After specimen preparation, assembly of the specimen cage was prepared via which the specimens were hung on site. This was an important step in this study as the assembly must be durable while, at the same time, easy to handle. First, the top and bottom surface of the specimens were covered with Byute Flash®, a thick rubber/butyl adhesive aluminium tape, to avoid multi-directional exposure of specimens. Figure 2 shows the sealing of the specimen top and bottom surfaces for unidirectional exposure.

Next, high-tensile strength plastic nets with chemical resistance were cut in such a way that the specimens are completely contained inside. For safety, two nets were used for each specimen. Figure 3 shows the net assembly for hanging of the specimens after sealing the top and bottom with the aluminium tape.

After that, a hanging assembly was made using a 2 mm durable stainless steel wire with swages to connect them with the top side of net. Considering the site conditions, 0.75 m long wires were cut for each specimen; after swaging the wire on both ends the total length remaining was 700 mm. Figure 4, shows the swages on top and bottom of the wire and the total assembly before hanging.

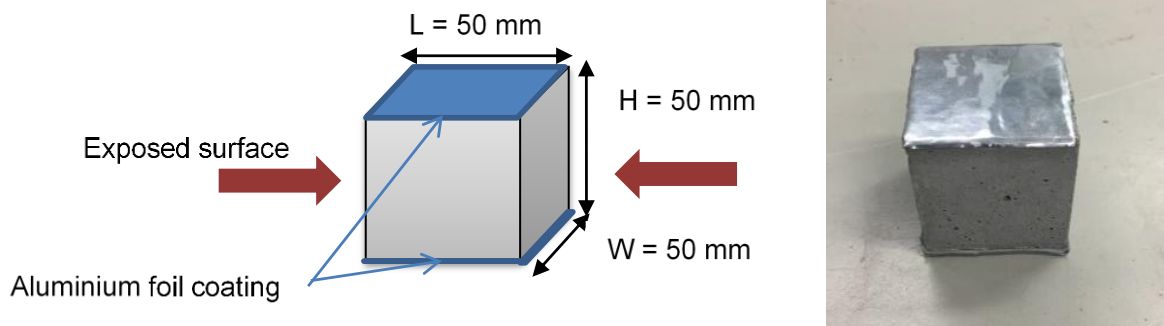


Figure 2. Specimen to be sealed for exposure condition.

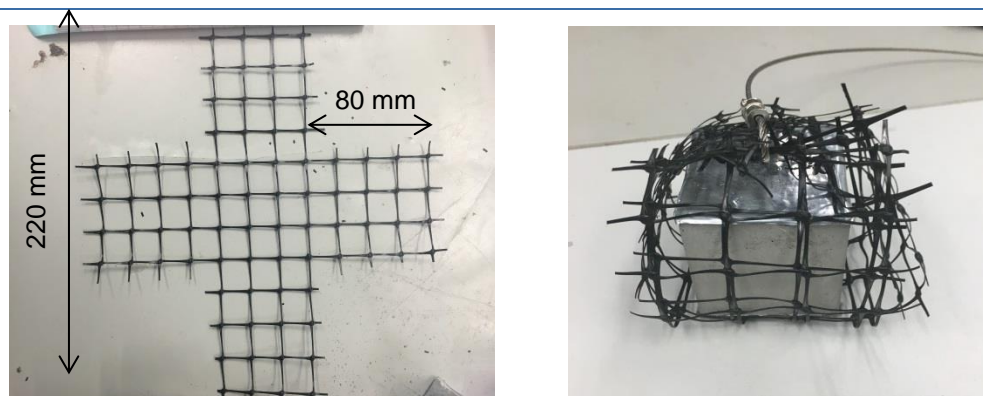


Figure 3. Net assembly for hanging specimens: dimensions (left) and after construction (right).




(a) Top swage for attachment to connecting line. (b) Bottom swage connection to net basket. (c) Specimen hanging.

Figure 4. Specimen with the net assembly ready to be placed on site.

Colours we associated with each mortar type of FA-GPm, AASm, SRPCm, CACm and MM for better identification on site. FA-GPm specimen had a white tag, AASm black, SRPCm red, CACm blue and MM a yellow tag. Coloured tapes were rolled on the top and bottom swage of each specimen for identification with serial number of the specimen written over it (see Table 4).

Table 4. Tag colour coding.

FA-GPm	
AASm	
SR	
CAC	
MM	

## 4.2 Site location

Sydney Water's North Head Wastewater Treatment Plant (WWTP) in Manly, Sydney, Australia, was selected for running of this long-term experiment. Figure 5 shows an aerial view showing different site locations. This is the second largest WWTP in Sydney running 24 hours a day, 7 days a week.

## 4.3 Atmospheric condition assessment

There were 3 digesters used for the study (see Figure 5). Figure 6 shows the digesters and the

small overflow chambers. The specimens were hung inside the overflow chambers of the three digesters for the comparative study. To understand the severity of the environment present inside these digesters, the atmospheric concentration of hydrogen sulphide ( $H_2S$ ) and temperature was recorded for a period of 13 days before the placement of the specimens and throughout the entire experimental duration. An Odalog gas logger was used for this purpose and data was saved at intervals of five minutes. Figure 7 shows the gas monitoring system placed in the digester sewage drain.

## 4.4 Placement of specimens in digester

The specimens were hung in each digester drain by seven 5 mm thick stainless steel wires drilled in the shorter dimension (975 mm at the centre) of the drain housing walls. The distance between each stainless steel wire was kept constant and is equal to 175 mm. Similar mortars were placed from left to right in each digester starting from FA-GPm on wire 2, then AASm, CACm, SRPCm and, finally, MM on wire 6 towards the right. Each wire supports 10 specimens of each type. Digester 1 contains serial # 1 to 10 for each type of mortar specimens, Digester 2 contains serial # 11 to 20 and Digester 3 contains serial # 21 to 30. Figure 8 shows the hanging pattern and schematics of different specimens in each digester.



Figure 5. Aerial view of North Head Wastewater Treatment Plant showing digesters 1 to 3.



(a) Digester 1 (left) and 3 (right).



(b) Digester 2 drain, where specimens were placed.

Figure 6. Digesters at site for hanging the specimens.

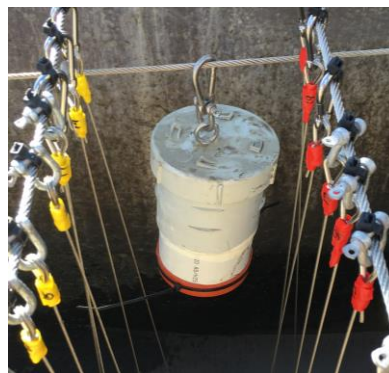
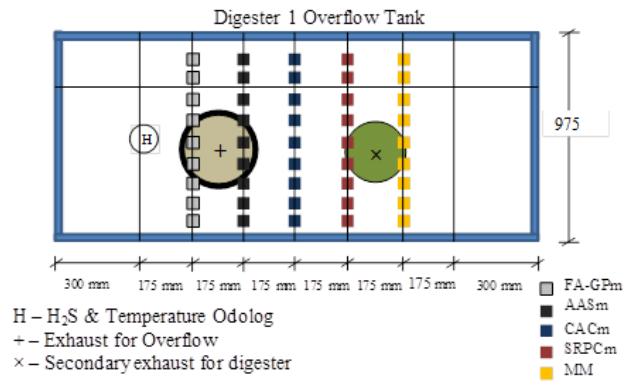


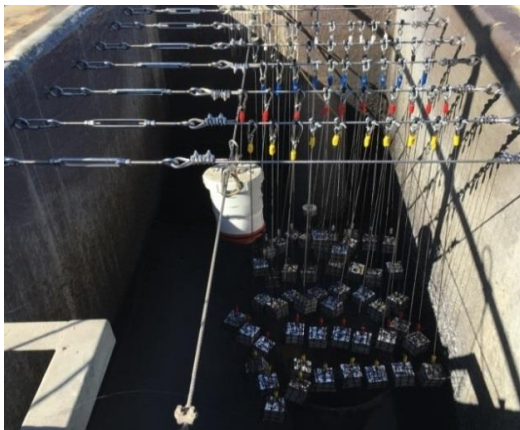
Figure 7. Left: OdaLog data logger placed inside the drain for measuring H<sub>2</sub>S concentration and temperature. Right: Specimens placed inside of drain.



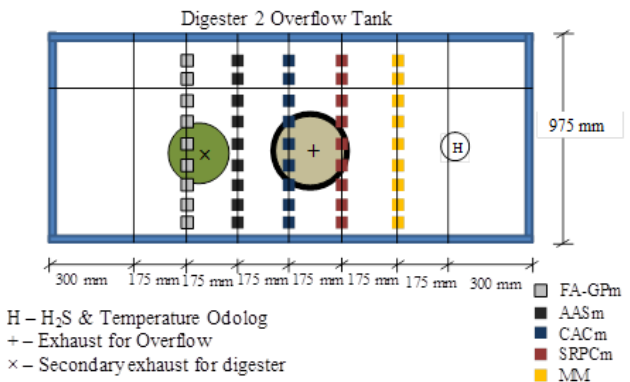
(a) Specimen hung in Digester 1



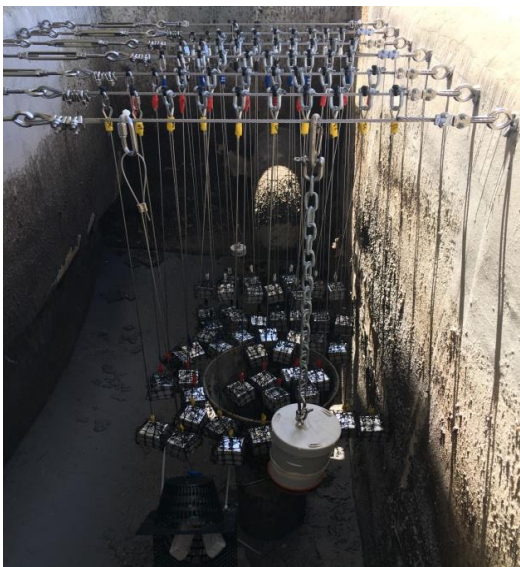
(b) Schematics of Digester 1



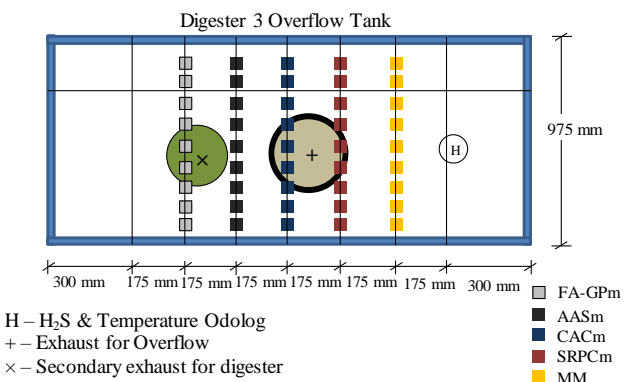
(c) Specimen hung in Digester 2 (lined with MM product in June 2014)



(d) Schematics of Digester 2



(e) Specimen hung in Digester 3



(f) Schematics of Digester 3

Figure 8. Specimen's hanging pattern in each digesters.

#### 4.5 Characterization of the environmental conditions

The maximum H<sub>2</sub>S gas concentration per day is shown in Figure 9(a); Figure 9(b) gives the average H<sub>2</sub>S gas concentration per day for the three-year period from the start of the experiment. The long-term estimation of the average H<sub>2</sub>S gas concentration in Digester 1 years 1, 2 and 3 years was 20 ppm, 53 ppm, and 48 ppm, respectively. Similarly, for Digester 2 these values were 19 ppm, 1.5 ppm and 1.0 ppm, and for Digester 3 17 ppm, 27 ppm and 29 ppm.

Daily maximum H<sub>2</sub>S gas concentrations were up to 880 ppm, 514 ppm and 706 ppm in Digesters 1, 2 and 3, respectively, whereas a daily average H<sub>2</sub>S gas concentration were up to 195, 102 and 228 ppm. It was observed that the H<sub>2</sub>S variation depends upon the activeness of the digester and time of the year. This long term estimation of atmospheric conditions confirmed that digesters 1 and 3 were adequate to maintain the corrosive environment throughout the exposure period, exceeding the concentration (10 ppm) required to sustain sulfuric acid generation [22]. However, some periods with low H<sub>2</sub>S gas concentrations were also observed. Overall, the overflow chamber of digester 1 was much more aggressive compared to digesters 2 and 3.

Figure 9(c) shows the change in daily average temperature for 36-month duration, which varies from 12.7°C to 33.5°C in all the three digesters. This rise and fall of temperature inside the overflow chamber were due to atmospheric rise and fall within different times of the day, outside weather condition and the temperature of the gas coming from the anaerobic digester.

Wells et al. [46] found humidity, in addition to temperature and H<sub>2</sub>S concentration, also affects the rate of concrete corrosion in sewers. Attempts to measure the relative air humidity inside the overflow tanks were made but failed to produce reliable readings, with some loggers failed within a few days after installation. However, visual observations made during sample extractions found that the samples inside the tank with highest H<sub>2</sub>S gas concentration has highest moisture content i.e. saturated, and the samples inside the tank with the lowest H<sub>2</sub>S gas concentration has the least moisture content i.e. dry.

#### 4.6 Specimen collection and analyses performed

Sampling of specimens from the two different digesters was undertaken after 6, 12, 24 and 36 months of exposure. The specimens were separated from the net and placed in an airtight plastic bag designating the type of mortar, location of the specimens and reference number. Continuous monitoring of H<sub>2</sub>S concentration was carried out to safely remove the specimens. This extraction was performed as per the extraction method explained by Herisson et al. [13, 23] and Kiliswa [24]. After the removal of organic slime from the surface, they were photographed to observe their visual variations and their surface pH was estimated. Afterwards, the plastic bags having specimens were sealed and stored in an insulated storage box to transport the specimens from the field to the laboratory for further testing.

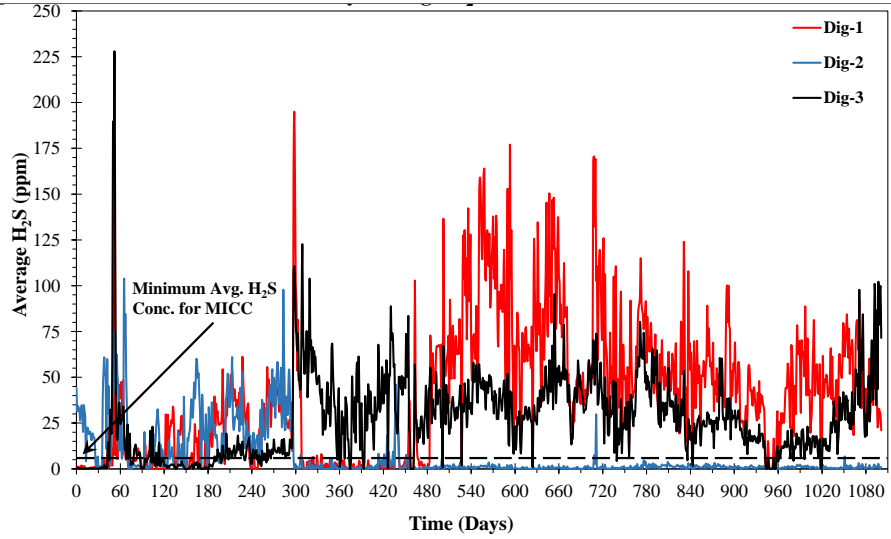
### 5 Experimental Results

After removing the specimens, they were taken to the Laboratory in the School of Civil and Environmental Engineering at University of New South Wales (UNSW), Sydney. Initially, they were removed from the net in which they were placed and washed to remove dry slime and surface organic matter. They were placed in an oven for 24 hours in the lab to remove the excess water from the concrete. Then the specimens were cooled to room temperature and the weight of the specimen measured and compared with the initial weight.

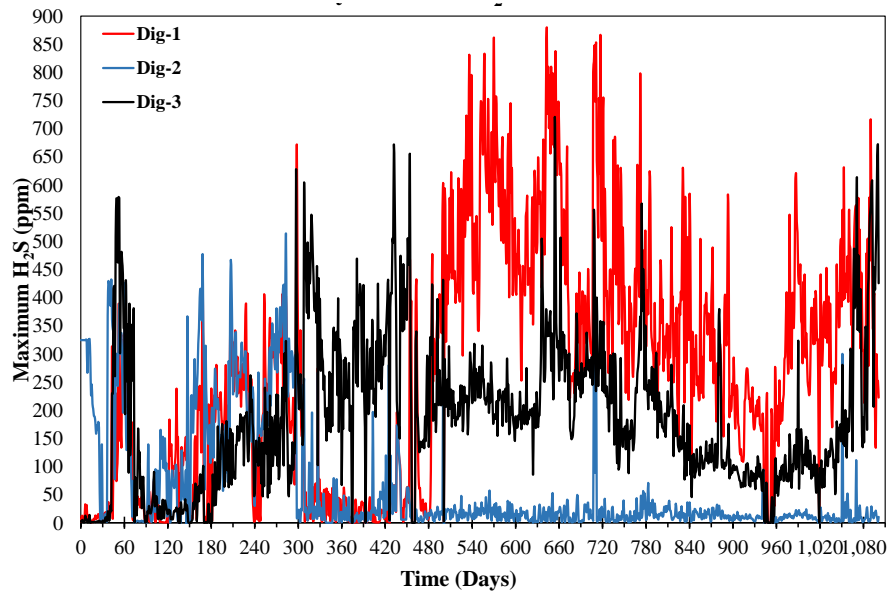
To monitor the bio-deterioration of all mortars, the following investigations were undertaken:

- visual observations;
- change in weight;
- change in compressive strength;
- variation in surface pH;
- depth of neutralisation;
- pH profile;
- x-ray diffraction to determine transformation of products during the degradation; and
- SEM images with EDS mapping formorphological and microstructural changes.

Daily Average H<sub>2</sub>S concentration (ppm)



Daily maximum H<sub>2</sub>S concentration (ppm)



Average daily temperature

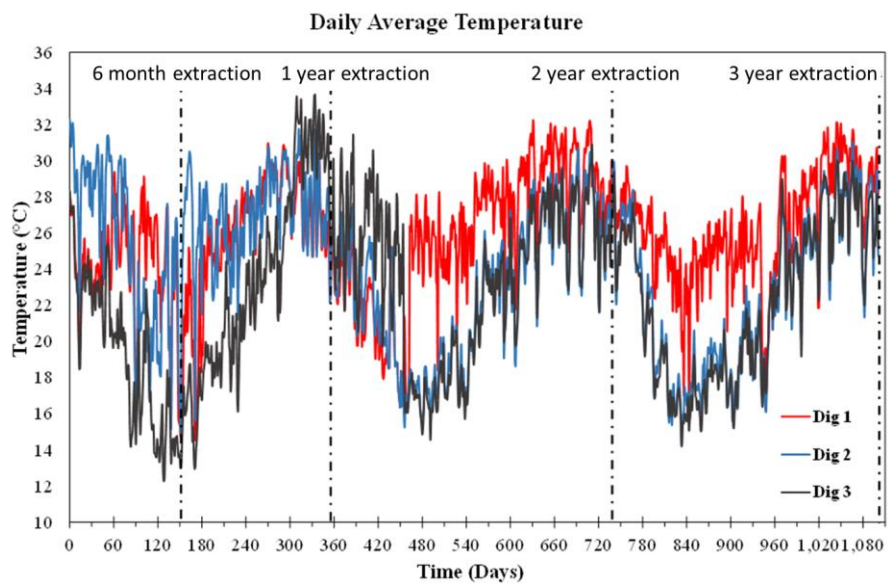


Figure 9. Environmental conditions in each digester.



## 5.1 Visual observations

The physical assessment of all five types of mortar from the three digesters included assessment of surface deterioration, loss of material, colour changes, efflorescence, cracking and crazing. Table 5 shows the FA-GPm, AASm, CACm, SRPCm and MM specimens after 12, 24 and 36 months of exposure from all three digesters.

No major signs of physical deterioration such as cracks, or spalling were observed on the surface of FA-GPm and CACm after 12 months of exposure. However, major colour changes were observed in all specimens at the exterior exposed surface. In case of SRPCm, MM and AASm whitish efflorescence was observed on the surface, which might be due to initial carbonation and/or H<sub>2</sub>S acidification in the environment, which is considered to be the first step in the degradation of concrete when exposed to MICC [25]. The surface assessments

indicated that specimens extracted from digester 1 were more severely deteriorated compared to other digesters. After 24 months, the loss of surface material extracted from digester 1 varied between 1 and 3 mm for AASm, and 2 and 3 mm for SRPCm. After 3 years of exposure, this loss was around 7 mm for SRPCm. The AASm specimens also experienced major reduction in dimension with extensive cracking throughout causing complete disintegration of specimen. FA-GPm and CACm specimens also experienced some minor surface deterioration and aggregate pop-out; however, no major disintegration and loss of cubical shape was observed in the specimens from all three exposure conditions. The MM specimens initially after 12 months only experienced some efflorescence, however after 24 and 36 months of exposure, minor cracking and loss of around 1 to 2 mm surface material was observed, especially after exposure to the conditions of digester 1.

Table 5a. Visual observations after 6, 12, 24 and 36 months of exposure: FA-GPm specimens.


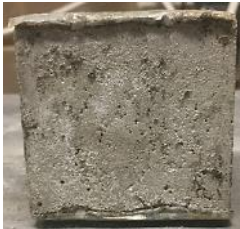







Specimen Type	Exposure Period	Dig - 1	Dig - 2	Dig - 3
FA-GPm	12 months			
	24 months			
	36 months			

Table 5b. Visual observations after 6, 12, 24 and 36 months of exposure: AASm specimens.










<b>AASm</b>	12 months			
	24 months			
	36 months			

Table 5c. Visual observations after 6, 12, 24 and 36 months of exposure: CACm specimens.










<b>CACm</b>	12 months			
	24 months			
	36 months			

Table 5d. Visual observations after 6, 12, 24 and 36 months of exposure: MM specimens.
















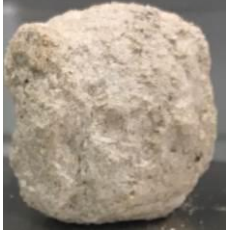


<b>MM</b>	12 months			
	24 months			
	36 months			

Table 5e. Visual observations after 6, 12, 24 and 36 months of exposure: SRPCm specimens.

<b>SRPCm</b>	12 months			
	24 months			
	36 months			

## 5.2 Variation in mass and compressive strength

Specimen weights were taken after drying in an oven for 24 hours at 60°C. The change in weight was determined by comparing against initial weight measured at 28 days after casting. Figures 10(a) to (e) show the mass change for all five mortar types. After 6 months of exposure, some specimens showed a few percent gain in mass. This mass increase is variable depending on the mix; for example, the AASm gained around 0.2% in mass compared to MM that gained 2.4%. This was likely due to the uptake of water and organic matter present in the sewage and absorbed into the mortar's pore structure as the specimens were stored at 50% RH from 24 hours until testing [26].

After 24 months of exposure all specimens except for CAC showed loss in mass. FA-GPm and AASm also showed loss in mass with respect to the exposure duration, which may be due to the variation in microstructure as a result of reaction of NASH and CASH gels with sulphur in the digester atmosphere and diffusing within their microstructure.

The CACm specimen showed gain in mass, which may be linked with the formation of calcite ( $\text{CaCO}_3$ ) and secondary gibbsite ( $\text{Al}(\text{OH})_3$ ), from katoite ( $\text{C}_3\text{AH}_6$ ), as a result of carbonation and formation of stratlingite (a reaction of silica with CA) within the microstructure. This increases the mechanical properties and improves the density of the matrix [27]. The formation of sulphates, calcite, gibbsite and stratlingite also increases the overall mass of CACm hiding the effect of the slight surface deterioration that might occur.

It was observed that the mass gain in CACm was higher in digester 2 and 3 specimens, compared to that of digester 1. The loss of mass in FA-GPm, AASm, MM and SRPCm specimens was greater in specimens extracted from digester 1. Based on the assessment of physical properties, the deteriorations within the AASm and SRPCm mixes were more pronounced compared to that of FA-GPm, MM and CACm. Overall, the CACm mix showed a superior durability to that of the other mixes in all three digesters.

The variation in compressive strength of FA-GPm, AASm, CACm, SRPCm and MM after two and three years of exposure are shown in Table 6. The overall loss in strength with respect to reference compressive strength was greater in AASm and SRPCm, compared to the other three binders (FA-GPm, CACm and MM). This confirms that matrix deterioration in SRPCm and AASm was more pronounced. Moreover, the specimens placed in the overflow chamber of digester 1 experienced a greater loss compared to Digesters 2 and 3. After 36 months of exposure, the performance of the CACm mix was superior to the others, showing a 3–8% reduction in strength for specimens in Digesters 2 and 3, whereas the loss was 34% with exposure to Digester 1.

Calcium aluminate cement (CAC) undergoes a process of conversion, where the meta-stable hydration products of  $\text{CAH}_{10}$  and  $\text{C}_2\text{AH}_8$  are thermodynamically transformed into stable products of  $\text{C}_3\text{AH}_6$  and  $\text{AH}_6$ . The rate of conversion is influenced by temperature and humidity of the exposing environment. Consequently, the strength loss of the CAC samples would also be contributed by the conversion process of CAC and not only by the surface deterioration in sewer environment.

## 5.3 Porosity and dry bulk density

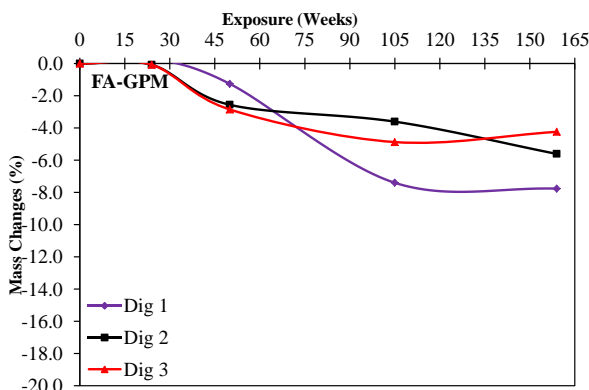
The volume of permeable voids and dry bulk density are shown in Table 7. The volume of permeable voids (VPV) of the FA-GPm and SRPCm reference specimens are reasonably comparable. As to are the results for the AASm and CACm specimens. The MM specimens had the lowest initial (reference) porosity.

The estimated VPV after exposure to infield deterioration included both sound and deteriorated matrix. In all cases the porosity after 36 months of exposure was slightly greater compared to 24 months, with the maximum porosities obtained from the specimens collected from digester 1. The FA-GPm, AASm and SRPCm mixes showed the higher porosities, while CACm and MM mixes lower porosities. It is acknowledged that the oven drying process included in VPV testing may have changed the porosity and microstructure.

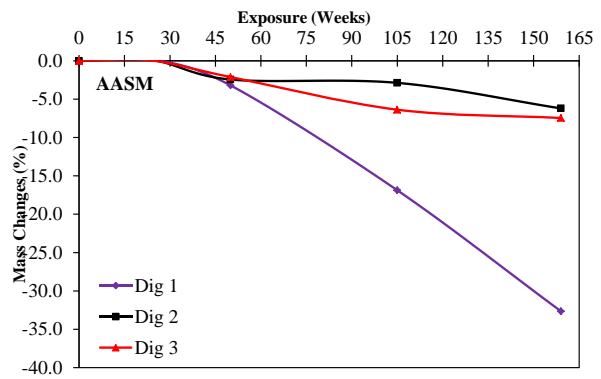
A reduction in dry bulk density was measured in FA-GPm, AASm, MM and SRPCm

specimens, indicating a loss of dry mass after exposure to the sewer environments; the loss of mass was also visually observed. In contrast, the CACm mortar specimens experienced a small reduction in porosity from 16% to 10~11%, and an increase in dry bulk density by 1.8%, 7.1% and 3.9% for digester 1 to 3,

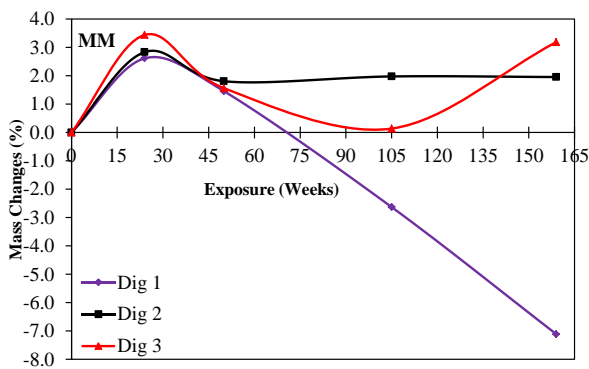
respectively. It was also found that the increment in porosity and loss in density was higher in the specimens extracted from digester 1, compared to the other two, confirming that severity of the environmental conditions affects the physical properties of the mortars.



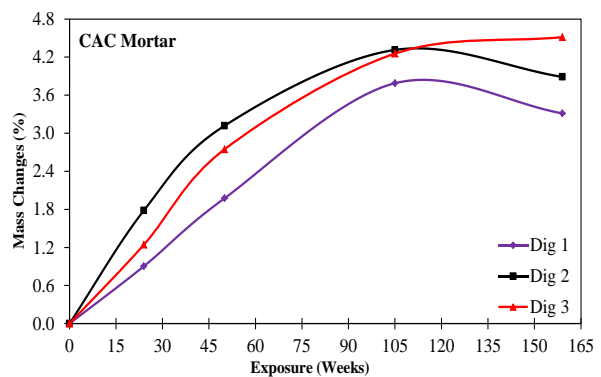
(a) FA-GPm



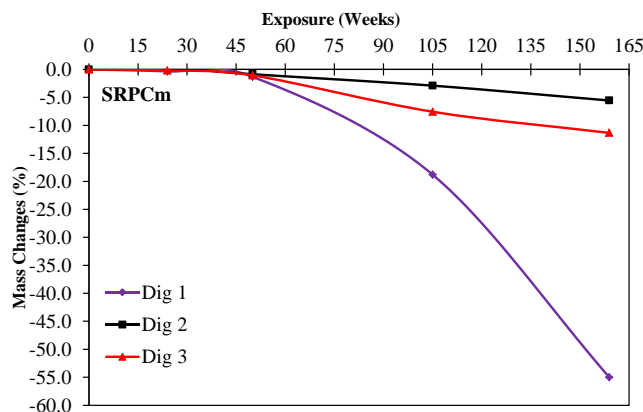
(b) AASm



(c) MM



(d) CAC



(e) SR Mortar

Figure 10. Variation in mass observed during 36 months of exposure.

Table 6. Compressive strength loss at 24 and 36 months.

Specimen Type	Exposure Duration	Compressive strength (MPa)			%age loss in strength		
		Dig. 1	Dig. 2	Dig. 3	Dig. 1	Dig. 2	Dig. 3
FA-GPm	Reference		47.8 ±1.6			-	
	24 months	22.3 ±2.4	42.9 ±1.9	29.1 ±3.6	53	10	39
	36 months	29.0 ±4.4	42.8 ±3.5	28.1 ±0.1	39	10	41
AASm	Reference		80.4 ±2.1			-	
	24 months	19.6 ±1.9	51.2 ±0.7	48.4 ±2.8	76	36	40
	36 months	0	38.2 ±1.4	27.7 ±1.8	100	52	66
CACm	Reference		56.3 ±1.8			-	
	24 months	38.3 ±1.7	52.6 ±2.6	52.1 ±3.6	32	7	8
	36 months	37.1 ±2.1	57.3 ±5.1	54.5 ±8.6	34	-2	3
SRPCm	Reference		50.7 ±1.7			-	
	24 months	15.9 ±2.3	27.9 ±2.9	22.2 ±2.1	69	45	56
	36 months	13.9 ±1.5	25.6 ±6.9	17.6 ±2.5	70	50	65
MM	Reference		64.1 ±1.9			-	
	24 months	22.1 ±0.2	41.6 ±1.2	28.3 ±2.9	66	35	56
	36 months	19.5 ±1.1	42.9 ±3.4	35 ±6.6	70	33	45

Table 7. Porosity and dry bulk density changes at 24 and 36 months.

Specimen Type	Exposure Duration	Porosity (%)			Dry Bulk Density (kg/m <sup>3</sup> )		
		Dig. 1	Dig. 2	Dig. 3	Dig. 1	Dig. 2	Dig. 3
FA-GPm	Reference		18.4 ±0.38			1717 ±9.8	
	24 months	27.9 ±0.07	22.5 ±1.3	19.9 ±0.1	1646	1667	1697
	36 months	27.7 ±0.3	24.8 ±1.1	26.1 ±1.4	1619	1630	1618
AASm	Reference		15.9 ±0.24			1932 ±7.6	
	24 months	22.3 ±1.3	19.6 ±0.5	19.9 ±0.0	1708	1848	1886
	36 months	28.1 ±2.3	20.1 ±3.5	19.7 ±0.2	1590	1859	1878
CACm	Reference		15.6 ±0.11			2037 ±3.8	
	24 months	10.6 ±0.9	10.1 ±0.3	10.9 ±0.2	2118	2074	2080
	36 months	11.9 ±1.7	10.6 ±0.9	11.9 ±0.4	2087	2183	2111
SRPCm	Reference		17.8 ±0.10			1893 ±0.2	
	24 months	23.4 ±1.06	20.6 ±0.3	21.3 ±1.1	1780	1828	1819
	36 months	24.8 ±3.6	21.3 ±1.1	21.0 ±5.1	1747	1811	1853
MM	Reference		12.3 ±1.1			1991 ±9.2	
	24 months	12.9±1.5	12.2 ±1.6	12.1 ±1.2	1915	1981	1957
	36 months	14.1±1.9	12.1 ±0.2	13.2 ±1.4	1885	1940	1909

## 5.4 Reduction in surface pH

In a hydrogen sulphide rich environment, surface pH is one of the important properties of concrete that influence the rate of corrosion and bacteria population growth [14, 25]. Changes observed in surface pH with respect to exposure time can be linked to the aggressiveness of the sewer environment and bacterial activity [28].

The surface pH of the specimens from each digester was determined and the results are plotted in Figure 11. The initial surface pH for the FA-GPm, AASm, CACm, MM and SRPCm mixes at 28 days of curing was 11.4, 12.6, 11.5, 12.6 and 12.7, respectively.

It is observed in Figure 11 that all five mixes experienced a major drop in surface pH during the first 6 months of exposure, followed by a further steady reduction until 36 months of exposure. The initial reduction in surface pH is linked to abiotic neutralisation (carbonation and acidification of H<sub>2</sub>S).

Previous experiments and analysis on MICC have shown that stage II of biotic growth and chemical corrosion initiates when the surface pH of specimen reduces below pH 9.0. The initiation of stage II is marked at a surface pH of 8.5 and is used to estimate the commencement of this stage with reference to exposure time for the five mortars exposed in all digesters. FA-GPm specimens reached the transition from stage I to II in a short exposure period of six months, compared to the other four mortars (AASm, CACm, SRPCm, and MM) that reached this transition after approximately one year of exposure. The rapid decline in surface pH of FA-GPm is linked to its lower initial pH and quicker matrix neutralisation, compared to the other mixes. This showed that the reduction in surface pH not only depends upon the environmental conditions but also on the type of mortar mix used.

Based on estimation of surface pH with respect to exposure time, it is observed that the performance of CACm in terms of percentage loss with respect to exposure time is higher than that of the others.

## 5.5 Depth of neutralisation and pH profile

Alkalinity of concrete is affected when exposed to an acidic environment. This leads to deterioration of the matrix and in case of reinforced concrete, to corrosion of reinforcement. The loss in alkalinity was estimated by spraying 1% phenolphthalein solution on freshly fractured surfaces of the mortar and measuring the pH profile. Regions having pH above 10 (depending upon the mortar type) turn a dark pink colour when phenolphthalein solution is sprayed. Dark pink, partially pink and colourless (neutralised) regions were observed and the pH profile compared for the exposed specimens. This provides an indication of the depth of dealkalisation due to the diffusion of acid or leaching of alkalis from the matrix [29, 30]. The colourless region corresponds to pH of around 8.2 to 11 depending upon the type of mortar.

The depth of dealkalisation after exposure was measured for the two directions from the surface; material loss of the exposed surface was included (added) in the dealkalised depth. Before exposure to the sewage environment, pH profiles of the reference mixes were determined; they were 11.8, 13.0, 11.9, 13.1 and 12.8 for the FA-GPm, AASm, CACm, MM and SRPCm mixes, respectively.

Figure 12 shows the coloured, partially coloured and colourless (neutralised) regions after spraying the 1% phenolphthalein solution on the freshly fractured mortar surface after 12, 24 and 36 months of exposure. OPC concrete usually displays a clear border between the coloured and colourless zones when sprayed with phenolphthalein indicator, with a narrow partially coloured region. In case of FA-GPm, however, the faded region was scattered throughout the depth. After 12 months of exposure, FA-GPm specimens from all three digesters were completely neutralised from all four sides making the depth of neutralisation equal to 25 mm. The depth of AASm, CACm, MM and SRPCm were 2 mm to 5 mm (see Table 8). All specimens showed an increase in average depth of neutralisation beyond 12 months of exposure.

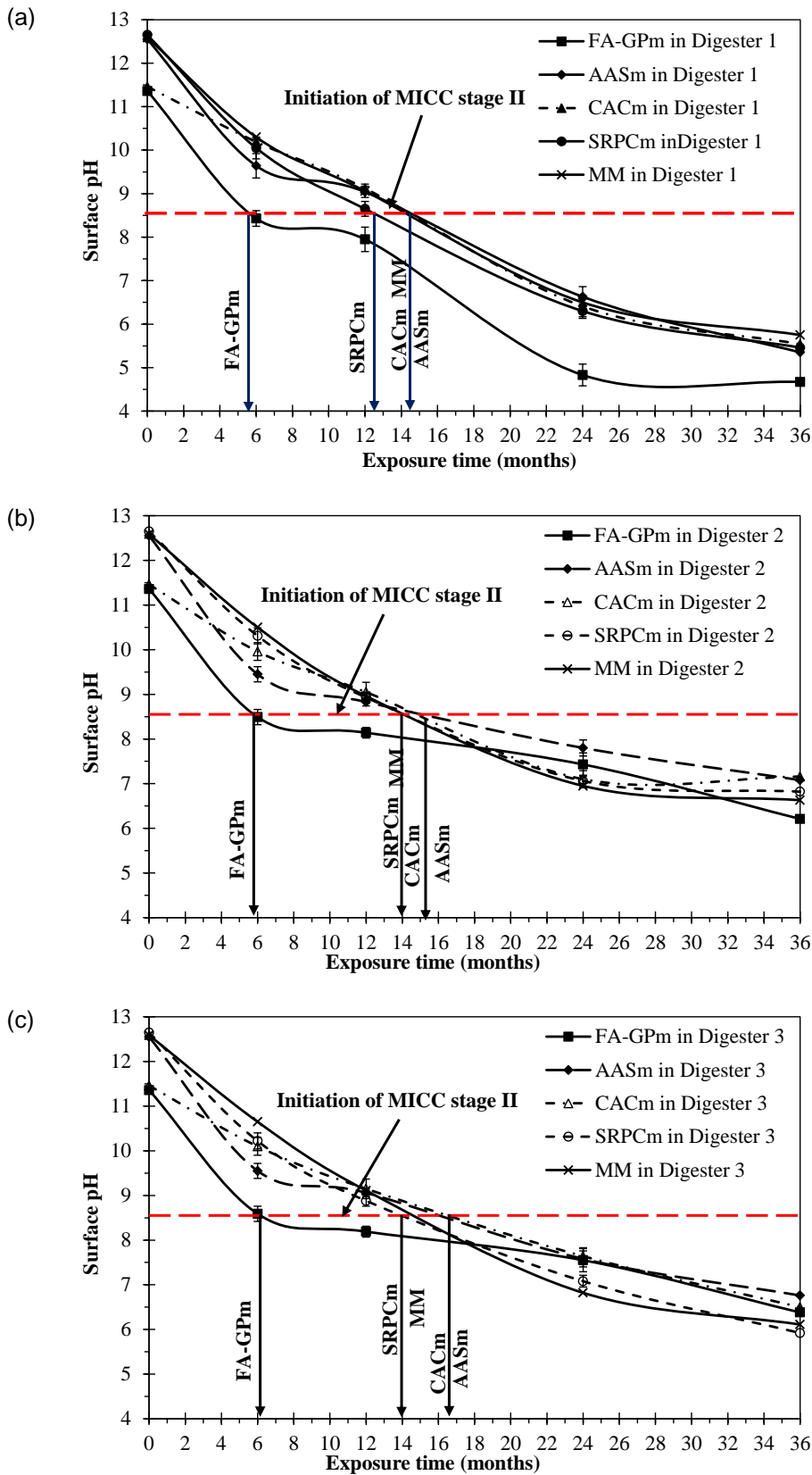
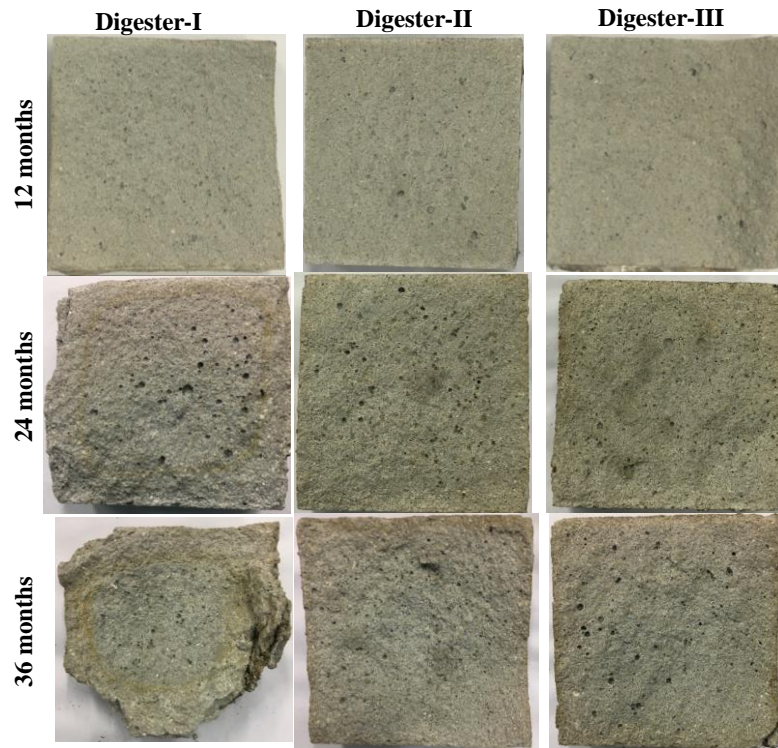


Figure 11. Variation in surface pH observed during 36 months of exposure: specimens from (a) digester 1, (b) digester 2 and (c) digester 3.



FA-GPm



AASm

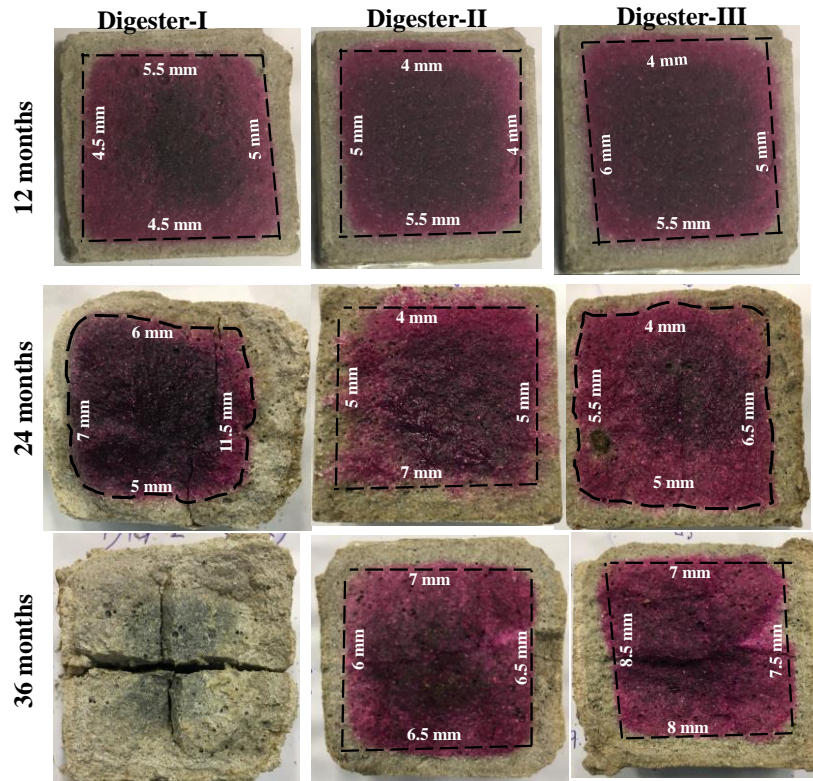
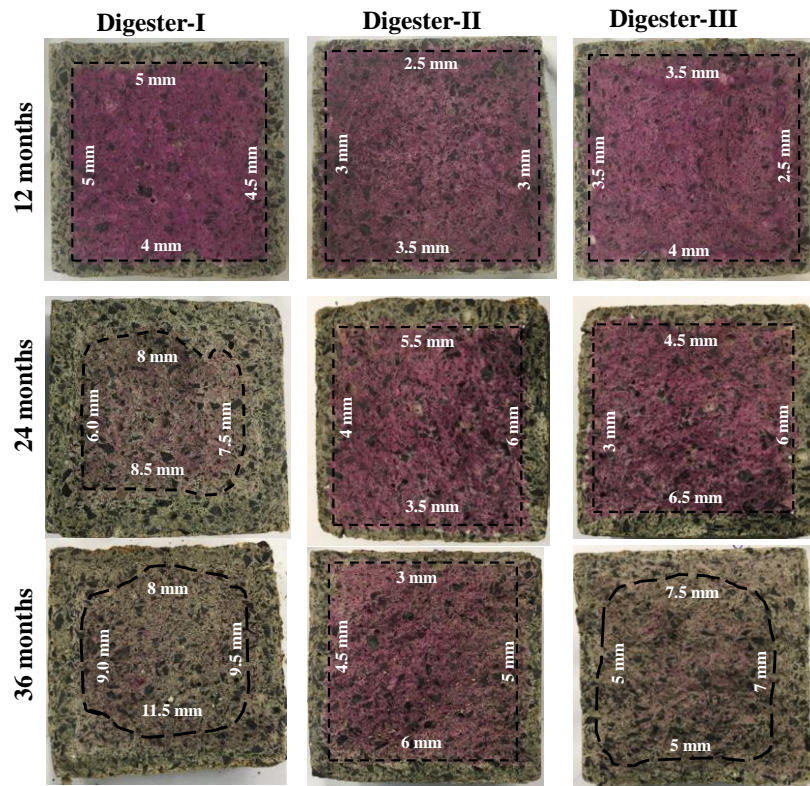


Figure 12. Neutralisation depth indicated by phenolphthalein.

**CACm**



**MM**

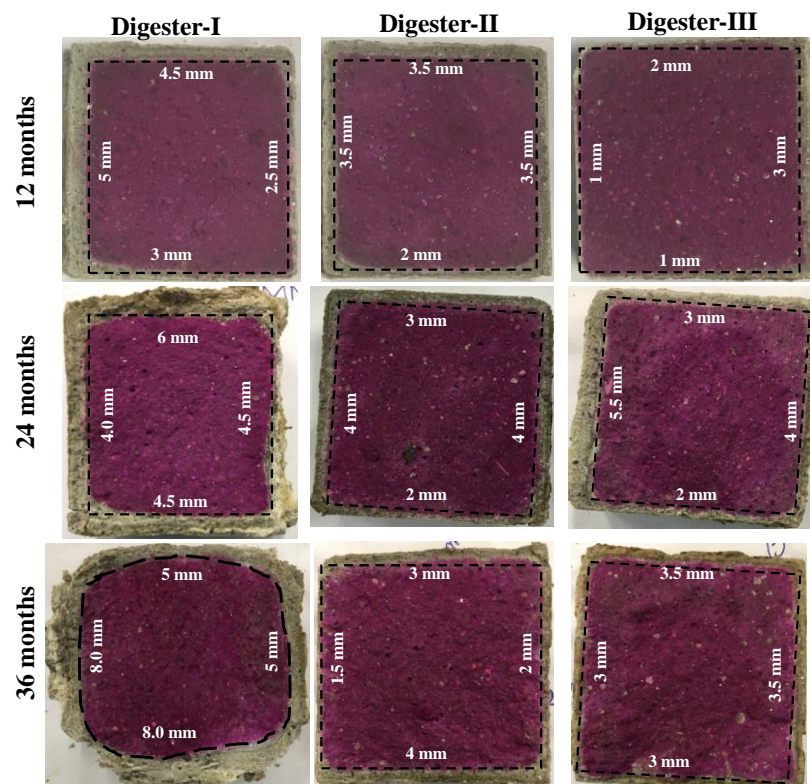


Figure 12. Neutralisation depth indicated by phenolphthalein (continued).

SRPCm

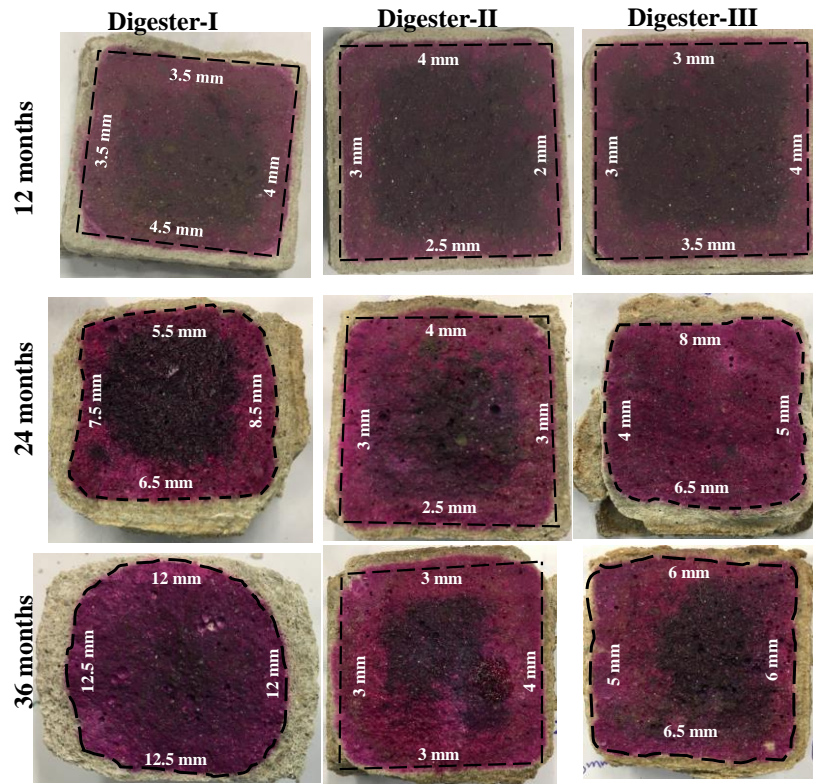


Figure 12. Neutralisation depth indicated by Phenolphthalein (continued).

The specimens collected from digester 1 indicated greater depth of neutralisation compared to those obtained from digesters 2 and 3. The increase in neutralisation depth in specimens can be linked to the rise in annual average H<sub>2</sub>S concentration which was much greater in digester 1, compared to digesters 2 and 3. Table 8, summarises the estimated depth of neutralisation for each mix design in all three digesters after 12, 24 and 36 months of exposure.

The pH of the mortar with respect to depth is used to investigate the occurrence of biogenic and chemical corrosion within the specimen as a result of exposure time. The pH of the specimen was investigated by the powder suspension method [31]. To obtain the pH profile, samples were cut into 3 to 4 mm thick slices starting from exposure surface and were grounded into a powder. To make the suspension solution

required to measure the pH, powder was first screened using 850 µm sieve, after which it was added into deionized purified water with a solid to liquid ratio of 1:1 and stirred for 5 minutes. The pH of the suspension was then measured using a calibrated pH probe from Labchem having a least count of 0.01.

Figure 13 shows the pH profile after 6, 12, 24 and 36 months of exposure for all three digesters. On the same graphs, change in colour chart of the phenolphthalein indicator over the considered range of pH values for all five mortar mixes is also presented. The un-carbonated pH value observed after 28 days of curing is also shown and the colourless pH value based on the literature presented. Based on the literature, the maximum pH in colourless region after carbonation is reported as well.

Table 8. Average depth of neutralisation after exposure to on-site conditions.

Specimen Type	Exposure Duration (months)	Dealkalisation Depth (mm)		
		Digester 1	Digester 2	Digester 3
FA-GPm	12 months	25	25	25
	24 months	25	25	25
	36 months	25	25	25
AASm	12 months	4.9	4.6	5.1
	24 months	7.4	5.2	5.2
	36 months	na	6.5	7.7
CACm	12 months	4.6	3.0	3.4
	24 months	7.5	4.7	5
	36 months	9.8	4.6	6.1
SRPCm	12 months	3.9	2.9	3.4
	24 months	7	3.1	5.9
	36 months	12.3	3.3	6
MM	12 months	3.8	3.1	1.7
	24 months	4.8	3.2	3.6
	36 months	6.5	2.7	3.3

Khan et al. [32] and Law et al. [33] estimated the pH of fully neutralised, colourless, region in FA-GP concrete to be around 10. Likewise, Noushini [34] estimated the colourless pH level for AAS concrete to be around 11. Based on previous research by George (1997) [35], the minimum pH of fully carbonated and converted CAC concrete varies around 11. A pH of 10.5 was estimated at the carbonation front which is selected to represent the region of fully carbonated CACm.

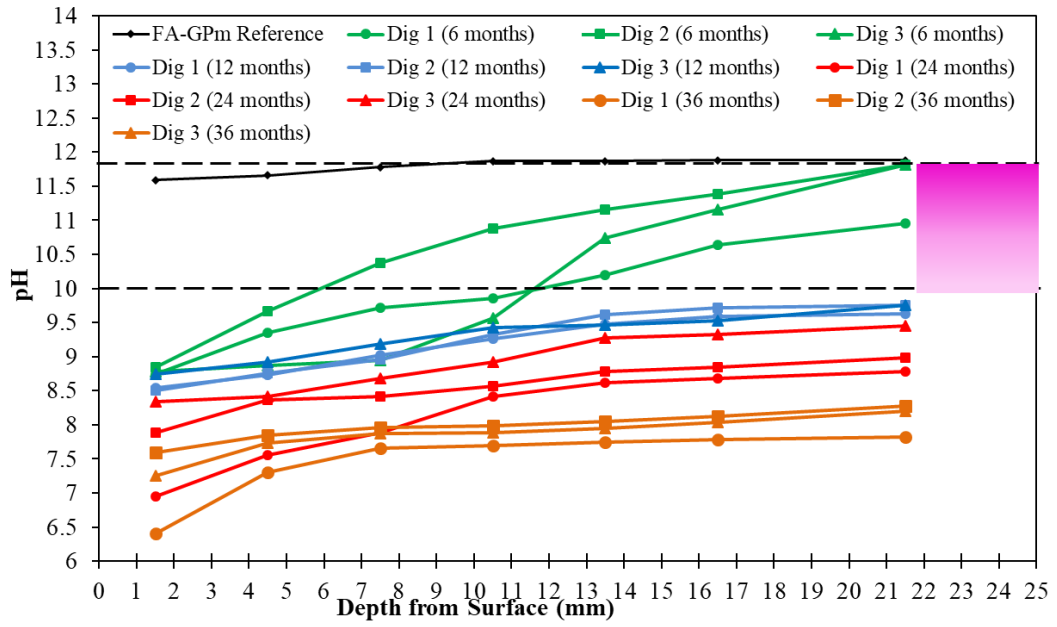
Research by Roy et al. [36], McPolin et al. [37], and McPolin et al. [38] measured the maximum pH after carbonation to be around 10 for Portland cement which was fully colourless. These pH values represent the smooth transition between fully neutralised colourless regions and intense pink/fuchsia colour zone and are marked in pH profiles of these four mortars. For the field conditions, the pH of FA-GPm specimens after 12 months of exposure dropped to less than pH 10 with a steady loss with respect to depth.

After 3 years, the minimum pH was estimated in FA-GPm specimen collected from digester 1 at around 6.4 within exposure region at 1.5 mm depth and then gradually increased to around 7.7 at the core. This depicts that the stage-II MICC has been initiated within the matrix of FA-GPm,

after abiotic neutralisation. AASm, CACm, MM and SRPCm specimens from each digester were also neutralised near the exposure region with pH below 11, 10.5, 10.5 and 10, respectively, after 6 months of exposure. It was also observed that with the increase in exposure duration from 6 to 36 months the pH of the bulk specimen near exposure was further reduced, irrespective of the digester. The slopes of these pH profiles indicate the depth up to which matrix was influenced after exposure.

Loss of surface material was experienced after 12 months of exposure. Moreover, by estimating the overall reduction in pH with respect to initial reference specimen after 36 months of on-site exposure, it was observed that CACm experienced 50% less pH reduction compared to other four mixes within the exposure region. This confirms a higher resilience of the CACm mix towards neutralisation due to simultaneous H<sub>2</sub>S acidification and carbonation, compared to the other three mixes. Further, pore blockage and reduction in porosity observed in CACm is linked to this higher performance of CACm, which may have reduced the diffusion of aggressive acid and carbon dioxide into the matrix and restricting the drop in pH.

**FA-GPm**



**AASm**

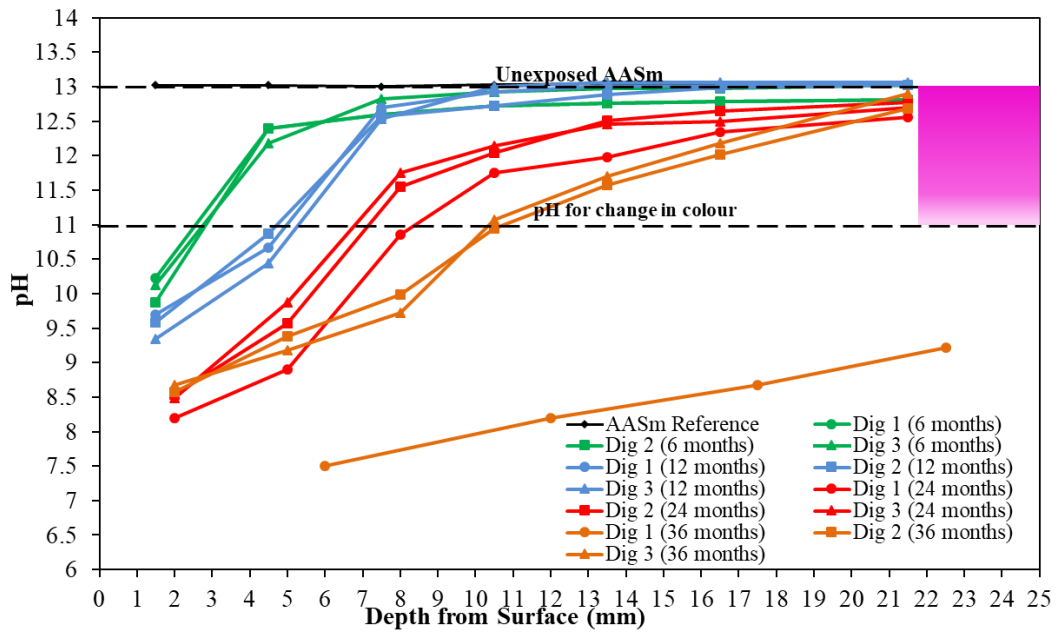
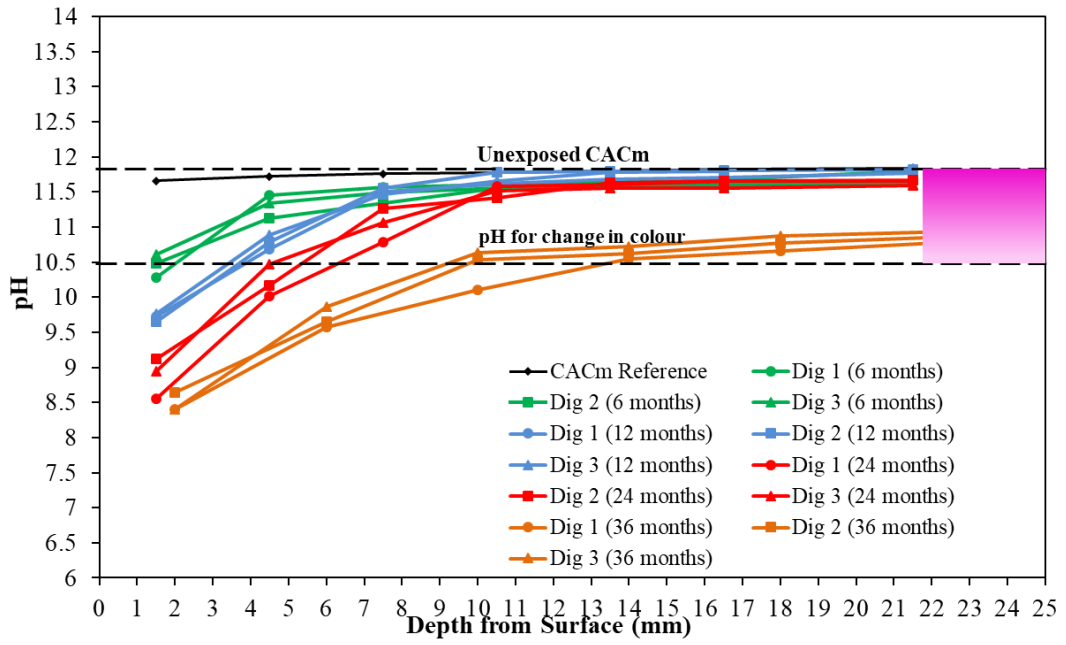


Figure 13. pH profile of specimens with respect to exposure duration and location.

**CACm**



**MM**

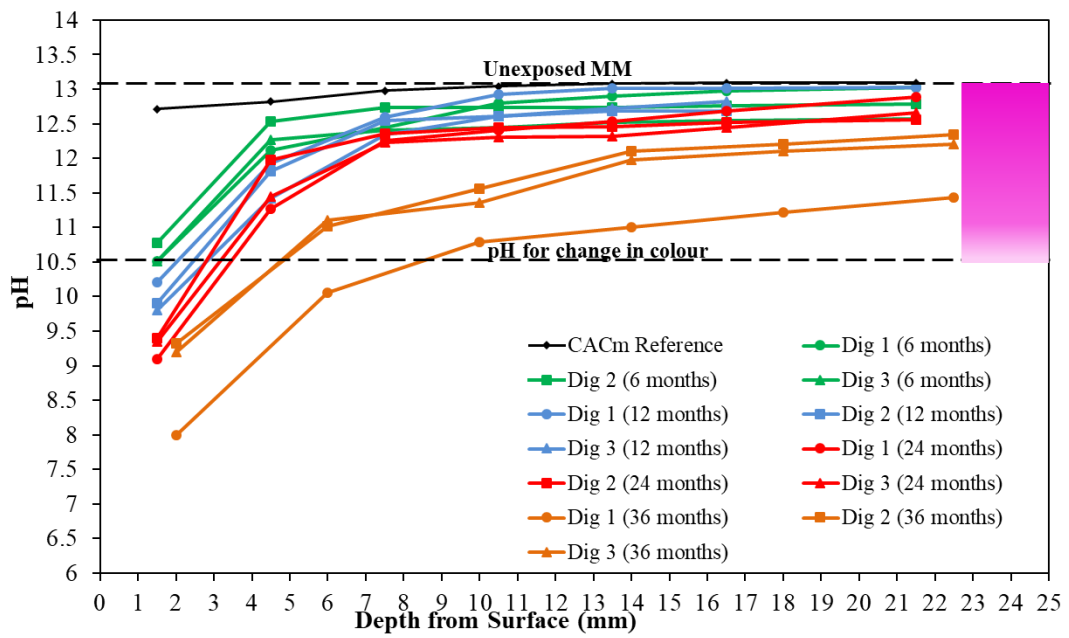


Figure 13. pH profile of specimens with respect to exposure duration and location (continued).

SRPCm

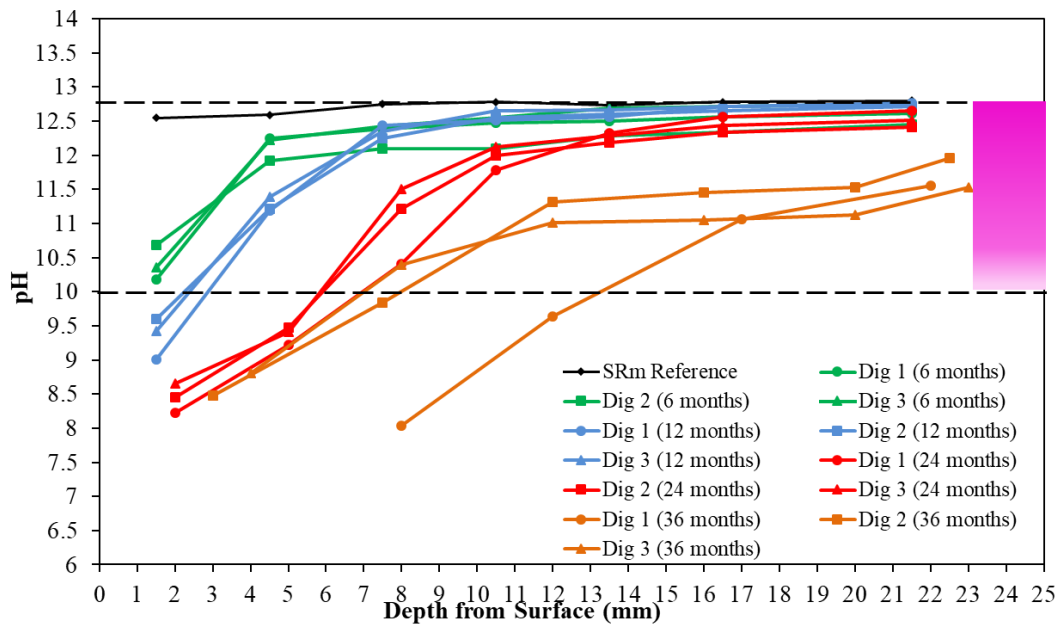


Figure 13. pH profile of specimens with respect to exposure duration and location (continued).

### 5.6 X-Ray diffraction analysis

The formation of new reaction products and different mineralogical phases within the eroded and uneroded matrix of the mixes was evaluated by performing XRD analysis. Samples were extracted at different depths from deteriorated specimen after 36 months of exposure to natural infield environment. These samples were pulverized using a grinder and analysed using the MPD (PANalytical) X'Pert Pro Multipurpose Diffractometer operated at 45 kV and 40 mA available at Solid State and Elemental Analysis Unit within the Mark Wainwright Analytical Centre at UNSW Sydney, Australia. The XRD patterns were obtained within the scan range of 5 to 70 and 0.026 2θ step size.

Further analysis and phase identification of the scan patterns were done using the X'pert High Score Plus software package. Since the mineralogical variations are the same in each digester for all five mortars, so the XRD patterns of specimens collected from digester 1 (most aggressive) are presented here.

Figure 14 shows the XRD pattern of FA-GPm with respect to depth from exposure surface (every 3 mm) after 36 months in the natural sewer environment of digester 1. Natron

( $\text{Na}_2\text{CO}_3 \cdot 10\text{H}_2\text{O}$ , PDF# 04-016-5072) at 16.5° and 29.6° and gypsum ( $\text{CaSO}_4 \cdot 2\text{H}_2\text{O}$ , PDF# 00-033-0311) at 11.7°, 20.8°, 29.1° and 31.2° were identified up to 25 mm and 18 mm depth from exposure, respectively. The broad peak of C-N-A-S-H at 29° was no longer identified up to 25 mm depth, indicating less resistance of this hybrid amorphous gel towards this aggressive sewer environment.

The XRD analysis of AASm after 36 months of exposure is shown in Figure 15, with reference to initial specimen before exposure. Prominent peak of gypsum was identified throughout 25 mm depth, indicating the decalcification of the amorphous gel matrix (CSH) and reaction of calcium with penetrating sulphate. In addition, the peak of calcite was also identified beyond 20 mm depth. Moreover, the formation of sodium sulphate was not observed anywhere in the AASm matrix. A slight hump of calcium silicate hydrate (C-S-H) (PDF# 00-033-0306) gel reappears beyond 20 mm in digester 1 with a prominent peak of gypsum. This indicates that the core matrix is not completely deteriorated with the crystallization of gypsum and poorly crystalline amorphous gel is still available to bind the fine aggregates within the matrix.

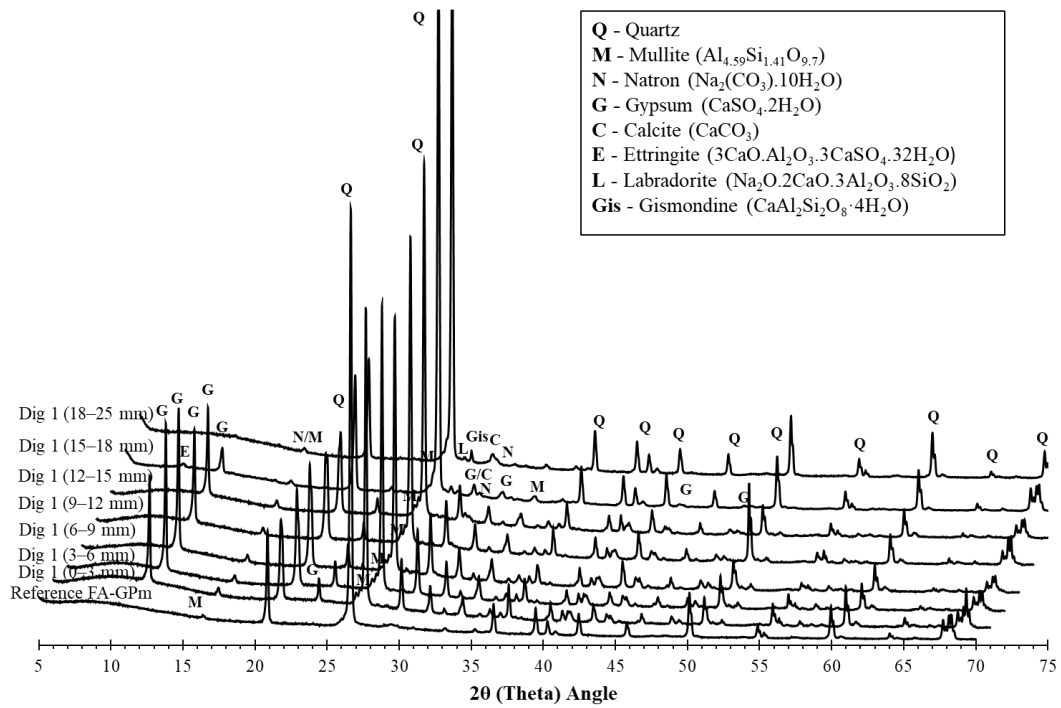


Figure 14. XRD pattern of FA-GPm after 36 months of exposure in digester 1.

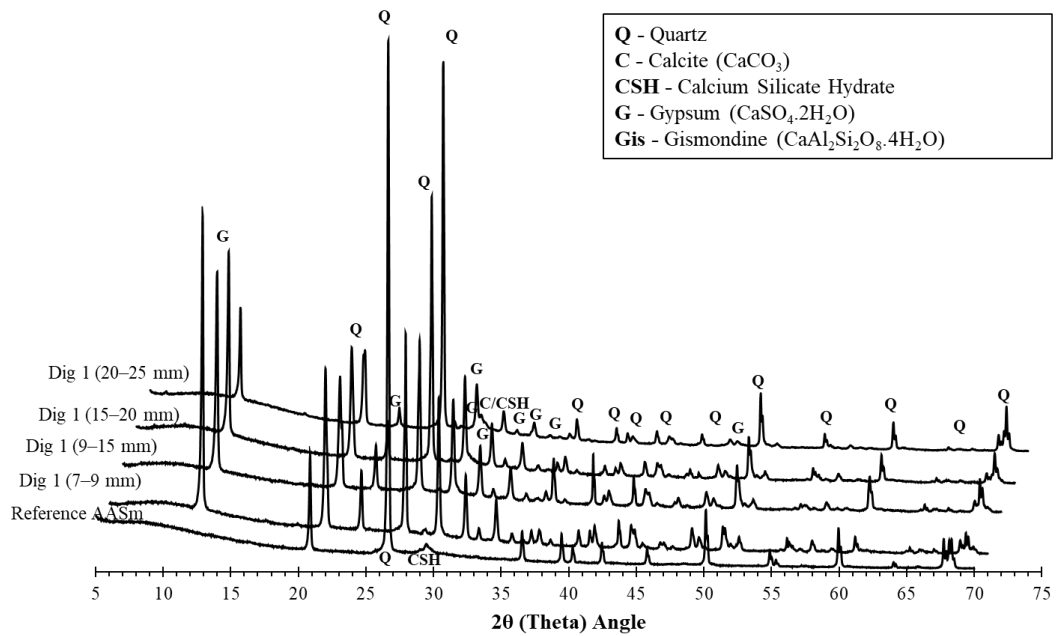


Figure 15. XRD pattern of AASm after 36 months of exposure in digester 1.



Figure 16 shows the XRD pattern of powder samples extracted from CACm after 36 months of exposure from corroded region (up to 4 mm) and core matrix (from 12 to 20 mm). The initial hydrates produced in the reference specimen include katoite ( $3\text{CaO}\cdot\text{Al}_2\text{O}_3\cdot 6\text{H}_2\text{O}$ , PDF# 01-76-2505)  $\text{C}_3\text{AH}_6$ , Gibbsite ( $\text{Al}(\text{OH})_3$ , PDF# 00-12-460)  $\text{AH}_3$ , monocalcium aluminate ( $\text{CaO}\cdot\text{Al}_2\text{O}_3$ , PDF# 04-10-5400) CA, and mayenite ( $12\text{CaO}\cdot 7\text{Al}_2\text{O}_3$ , PDF# 04-19-1284)  $\text{C}_{12}\text{A}_7$ , with some minor traces of mullite ( $\text{Al}_6\text{Si}_2\text{O}_{13}$ , PDF# 04-016-1588).

After in-field exposure, calcite due to carbonation and gypsum ( $\text{CaSO}_4\cdot 2\text{H}_2\text{O}$ , PDF# 00-033-0311), ettringite ( $3\text{CaO}\cdot\text{Al}_2\text{O}_3\cdot 3\text{CaSO}_4\cdot 32\text{H}_2\text{O}$ , PDF# 04-11-5267) due to sulphur penetration within the matrix was observed within the matrix. Formation of these minerals leads to the dissociation of katoite and formation of gibbsite.

The crystallization of calcite was observed up to 20 mm depth; whereas, the presence of gypsum and ettringite are limited to 12 mm. The peak of gibbsite was also identified within the corroded region (up to 4 mm), indicating that  $\text{AH}_3$  have not experienced the dissociation to monomer  $\text{Al}^{3+}$ , since the pH is well beyond 4.0 required for its disintegration. In addition, stratlingite ( $2\text{CaO}\cdot\text{Al}_2\text{O}_3\cdot\text{SiO}_2\cdot 8\text{H}_2\text{O}$ , PDF# 00-29-285) was also identified at  $7.1^\circ$  on XRD pattern; however, the presence of this phase was observed beyond 4 mm and to the maximum depth analysed of 20 mm. This mineral is formed as a result of the reaction of monocalcium aluminate with silica and improves the density of the matrix [27].

In addition to gypsum and ettringite, Ye'elimite ( $3\text{CaO}\cdot 3\text{Al}_2\text{O}_3\cdot\text{CaSO}_4$ , PDF# 00-33-256) was identified at  $23.6^\circ$  within 4 mm of depth in both digesters. This calcium sulfoaluminate may react with gypsum at higher humidity to form delayed ettringite and cause major deterioration to the matrix [39, 40].

The XRD analysis of MM after 24 months of exposure is shown in Figure 17 in comparison with the initial reference specimen. The XRD pattern of reference specimen (before exposure) shows the presence of Quartz ( $\text{SiO}_2$ , PDF# 01-85-796) at  $20.8^\circ$ ,  $26.6^\circ$ ,  $36.5^\circ$ ,  $50.1^\circ$  and  $60^\circ$ , Portlandite ( $\text{Ca}(\text{OH})_2$ , PDF# 01-73-8394) at  $18.9^\circ$ ,  $36.5^\circ$  and Calcium Silicate Hydrate (C-S-H) (PDF# 00-033-0306) gel at  $29.4^\circ$ . After 36 months of exposure, portlandite and CSH were completely disintegrated into gypsum within exposure region of up to 4 mm. Beyond 4 mm, peaks of ettringite ( $3\text{CaO}\cdot\text{Al}_2\text{O}_3\cdot 3\text{CaSO}_4\cdot 32\text{H}_2\text{O}$ , PDF# 00-13-350) and potassium calcium sulphate ( $\text{K}_2\text{Ca}_2(\text{SO}_4)_3$ , PDF# 04-08-8637) were identified within the matrix. These secondary sulphate mineral were not identified in the exposed corroding layer due to the fast thermodynamics of gypsum formation as reported by Davis et al. [41]. The peaks of primary binders (Portlandite and CSH) reappear at 12 mm depth. This indicates that beyond 8 mm depth the matrix is becoming stable.

Figure 18 represents the XRD pattern of SRPCm after exposure to aggressive sewer environment for the duration of 36 months in digester 1. The exposed region of almost 8 mm was completely disintegrated and was not considered in this estimation. The exposed region up to 10 mm showed extensive precipitation of gypsum and dissociation of primary hydrates which include Portlandite and CSH.

Prominent peak of gypsum was observed at  $11.6^\circ$  up to 19 mm depth in SRPCm. In addition, delayed ettringite was also formed and was observed at  $9.1^\circ$  beyond 13 mm depth as a result of the reaction of gypsum with mono-sulfoaluminate.

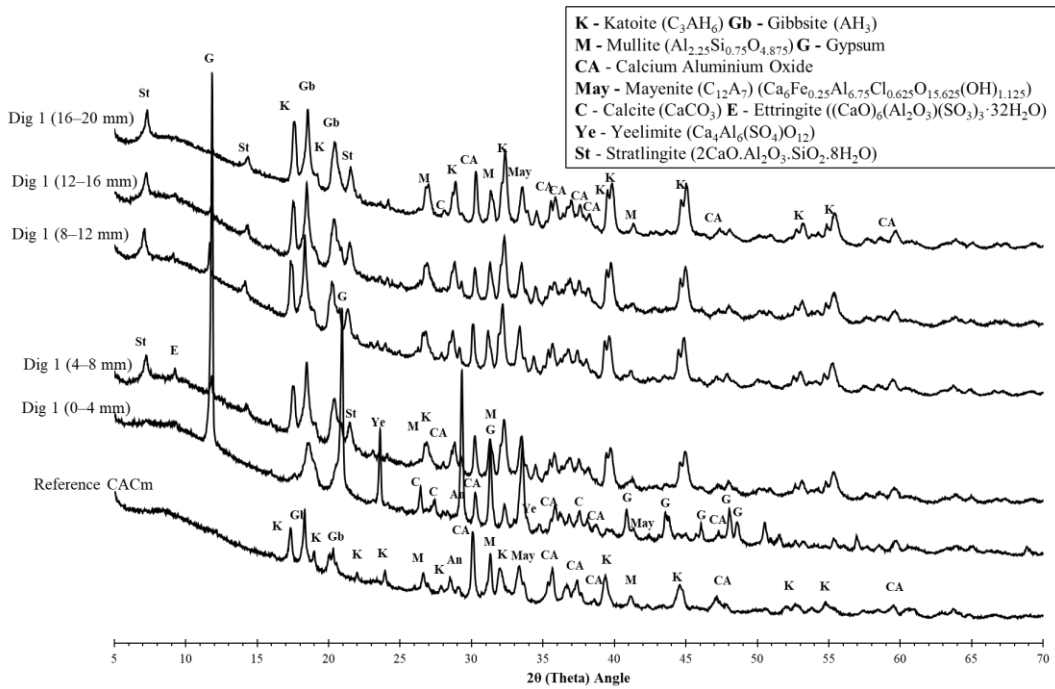


Figure 16. XRD pattern of CACm after 36 months of exposure in digester 1.

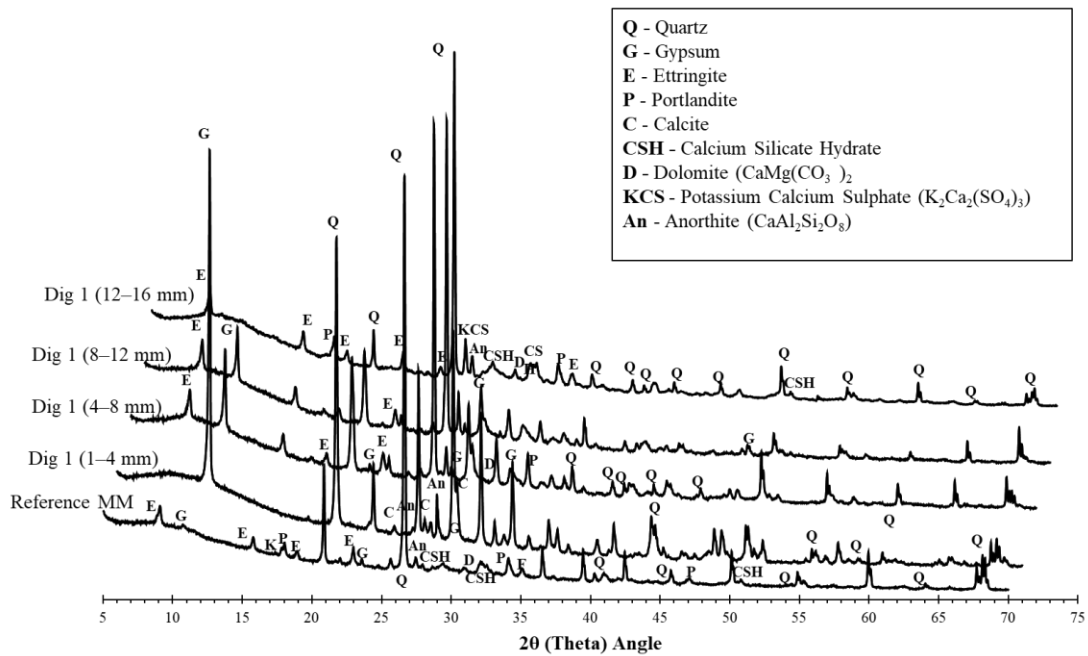


Figure 17. XRD pattern of MM after 36 months of exposure in digester 1.

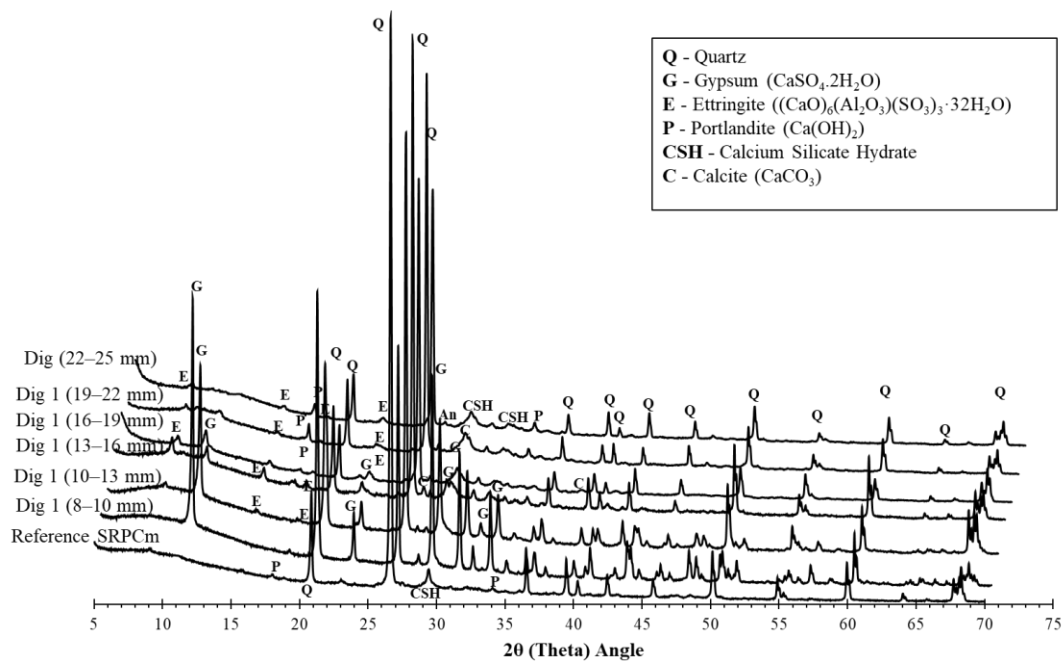


Figure 18. XRD pattern of SRPCm after 36 months of exposure in digester 1.

## 5.7 Scanning electron microscopy with EDX analysis

### SEM images of deteriorated region

The deterioration of the microstructure in terms of location of microcracks, interface between aggregate and matrix known as interfacial transition zone (ITZ) and morphological variations within the matrix and penetration of sulphate after exposure to natural sewer environment were investigated using SEM and EDX analysis. Figure 19, shows the microstructural variations of FA-GPm, AASm, CACm, MM and SRPCm extracted after 36 months from digester 1.

The matrix of low calcium FA-GPm specimens from each digester presents a dissociation of the binding gel matrix. It was observed that FA-GPm from digest 1 showed extensive porosity and permeable voids within the microstructure near the aggregate interface. Similarly, voids and gaps were also observed in the matrix of FA-GPm from digesters 2 and 3; however the porosity was much less. This rise in porosity results in the major loss in compressive strength and bulk density of geopolymer mortar. Beside the dissolution of geopolymer matrix, localized

crystallization of gypsum was also identified within the exposed region indicating the dissociation of hybrid N-(C)-A-S-H gel present in some locations.

After 36 months of exposure, AASm specimens extracted from each digester experienced major matrix degradation. Extensive crystallization of gypsum was observed within the matrix, which leads to the decalcification of C-A-S-H matrix. Development of cracks leading to an increase in meso-porosity was identified in the region with the precipitation of gypsum.

The matrix of CACm after 36 months of exposure showed localized regions of sulphate mineral with the development of micro-cracking. The initiation of hairline crack within the dense matrix was due to pressure generated from the crystallization sulphate mineral (gypsum and ettringite). However, this attack also resulted in the formation of AH<sub>3</sub> gel, which blocks the porosity and further diffusion of sulphate, hence improving the overall durability [42, 43]. This formation of amorphous gel within the matrix as a result of the dissociation of primary hydrates (katoite) also retains the physical properties and durable interface between matrix and aggregate.

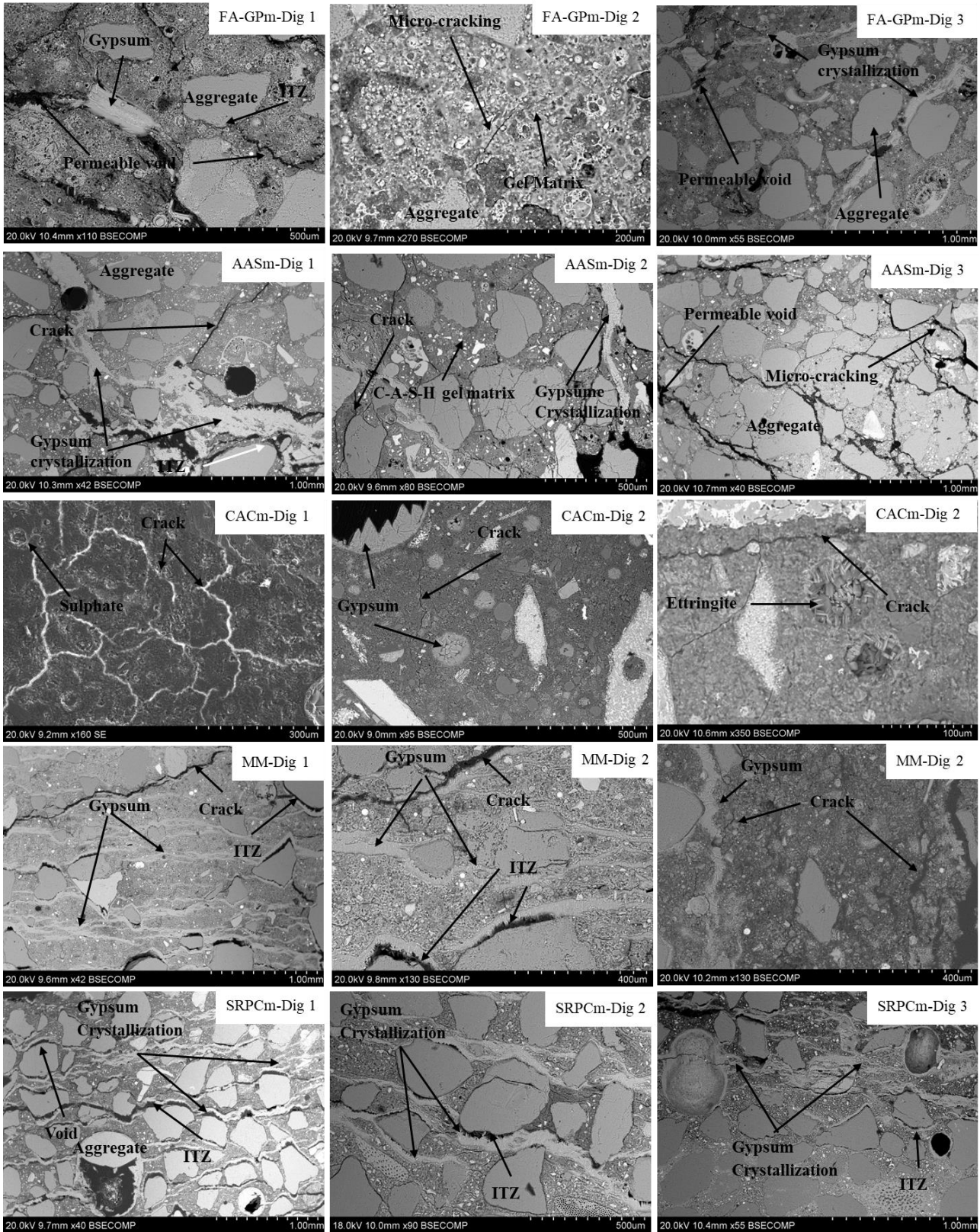


Figure 19. SEM images of deteriorated region within FA-GPm, AASm, CACm, MM and SRPCm after 36 months of exposure in each digester.

Comparing the microstructure of CACm specimen from each digester no extensive difference was identified in terms of morphological variations within the exposed matrix.

The microstructure of MM and SRPCm from each digester showed extensive crystallization of gypsum within the exposed matrix. This crystallization not only disintegrates the primary calcium-based hydrates but also reduces the durability of the binder by developing cracks. Moreover, the crystallization of these secondary minerals influences the ITZ region by weakening the bond between aggregate and gel matrix. These microstructural deteriorations observed within FA-GPm, AASm, CACm and SRPCm specimens extracted from each digester support the observations made in XRD analysis and variations estimated in physical properties such as mass, strength and porosity.

#### *Sulphur mapping with estimated depth of corrosion*

Sulphur mapping using EDX analysis after 36 months of exposure is presented in Figure 20. The penetration of sulphur within the deteriorated matrix is shown in red colour and the scale is provided to assist in estimating the depth of penetration within the microstructure. The penetration of sulphur in FA-GPm indicated localized regions of gypsum precipitation. The microstructure of FA-GPm from digesters 2 and 3 showed much denser matrix with much reduced crystallization compared to FA-GPm specimen from digester 1. The mapping of sodium (not shown here) indicated complete removal of alkali from the matrix of the geopolymer which leads to the major reduction in pH of the specimen.

The matrix of AASm showed extensive disintegration and crystallization of gypsum in red patterns within the matrix. This crystallization was much higher in AASm compared to FA-GPm due to much higher concentration of slag (high calcium content). The sulphate penetration within CACm matrix was observed as small

pockets of sulphate minerals (gypsum and ettringite). This crystallisation was observed in the CACm specimen from each digester and was more concentrated near exposure surface.

The mapping of MM and SRPCm showed extensive crystallization of sulphate minerals in the form of layers parallel to the exposure surface. This high sulphur penetration indicates the widespread deterioration of portlandite and C-S-H, increase in porosity and the extensive development of micro-cracks within the matrix. In addition, this indicates that stage II of MICC deterioration has initiated within the matrix. Moreover, the presence of sulphate within the matrix confirms that the microstructure was becoming comfortable for the growth of SOM and indicates oxidation of sulphate from H<sub>2</sub>S due to the bacterial activity [14, 44]. This bacterial action further drops the pH within the matrix, which is required to promote SOM growth [45].

SEM analysis with EDX mapping technique indicated the crystallization of gypsum and the overall depth up to which this mineral was identified. Multiple SEM with EDX analysis were performed to evaluate this deteriorated depth within FA-GPm, AASm, CACm, MM and SRPCm mortar after 36 months of exposure for each digester specimen. Table 9 represents the estimated average depth for each mortar type.

Table 9. Average depth of deterioration after 36 months of exposure to on-site conditions.

Specimen Type	Deterioration Depth (mm)		
	Dig. 1	Dig. 2	Dig. 3
FA-GPm	16.7	9.2	11.7
AASm	21.5	9.0	11.2
CACm	8.4	3.3	4.0
MM	11.0	3.5	4.6
SRPCm	17.9	8.5	9.5

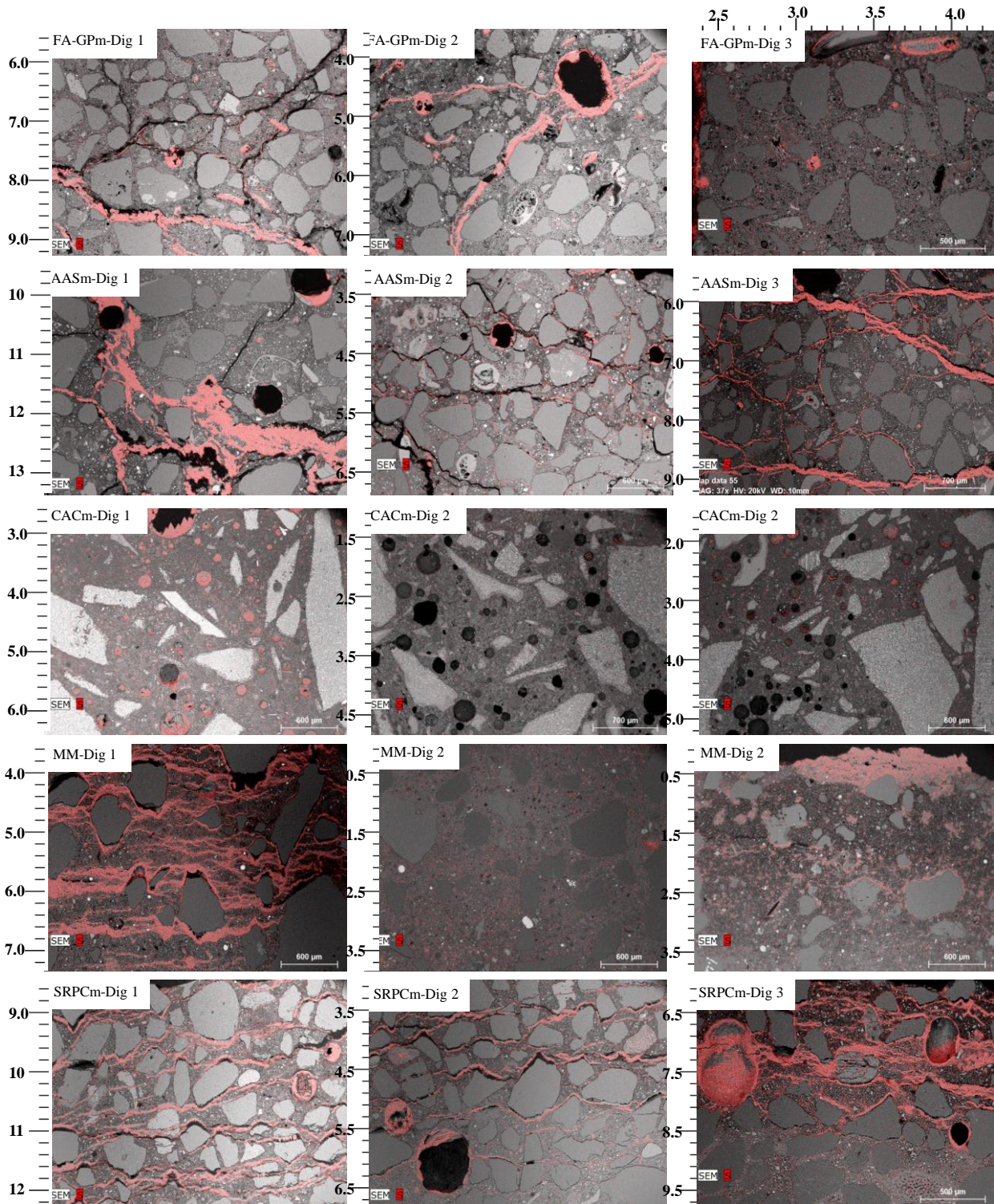


Figure 20. Sulphur mapping of deteriorated region within FA-GPm, AASm, CACm, MM and SRPCm after 36 months of exposure in each digester with.

## 6 Conclusions

Based on the test results and visual and physical analyses the following conclusions are drawn:

- Visual and optical microscope imagery after 36 months of exposure has shown structurally intact FA-GPm and CACm specimens with minor surface coarsening, whereas AASm and SRPCm experienced major deterioration with loss of surface material and crack propagation within the specimens. MM experienced the loss of around 2 mm of surface material.
- Some minor efflorescence was observed on the exterior surface of MM, SR and AASm, which is due to initial abiotic carbonation.
- Deteriorations within AASm and SRPCm specimens were more pronounced compared to FA-GPm, MM and CACm in terms of mass and strength. CACm showed gain in mass in all three digesters.
- Based on the assessment of visible deterioration, mass loss, strength reduction, porosity and bulk density, CACm showed good performance.
- FA-GPm and AASm specimens show a higher porosity compared to other mixes after exposure to the aggressive sewer environment in digester 1.
- Surface pH values and estimation of time required to initiate the stage II of MICC was less in FA-GPm compared to other three mortars. Moreover, increase in H<sub>2</sub>S concentration in natural sewer environment leads to a reduction of surface alkalinity and accelerates the commencement of MICC stage II.
- The depth of dealkalisation and reduction in pH was identified in FA-GPm compared to other mixes under sewer environments. The pH reduction after 24 months of exposure was lower in CACm compared to FA-GPm, AASm, MM and SRPCm, indicating resilience towards loss in alkalinity.
- X-Ray diffraction of each mortar revealed the crystallization of gypsum as the primary sulphate mineral within the matrix. The formation of gypsum was identified up to 18 mm, 25 mm, 12 mm, 12 mm and 19 mm depth from exposure surface within FA-GPm, AASm, CACm, MM and SRPCm specimens, respectively.
- SEM imagery showed the microstructural deterioration, crystallization of gypsum and weakening of ITZ between aggregate and binder. The precipitation of gypsum within the exposed region was more localized within FA-GPm and CACm compared SRPCm, AASm and MM.
- Mapping of sulphur indicated that the depth of deterioration was much greater in specimens extracted from digester 1, compared to digesters 2 and 3.
- The depth of deterioration within AASm and SRPCm was greater compared to commercially available CACm and MM after 36 months of field exposure in digester 1.

Lastly, it is concluded that the design of mix of binder systems is crucial in these very aggressive environments, and care is needed in translating these results to those of other, albeit similar, binder systems. Various combinations of source materials, of activators and the resulting microstructure will likely lead to differing results. Commercially available CAC products have a good track record. There is limited long term information on FA based geopolymer. The advantage of this programme is that it provides a direct contemporary comparison of the performance of different products.

# References

- [1] M. Alexander, A. Bertron, N. De Belie. Performance of Cement-Based Materials in Aggressive Aqueous Environments. Ghent: Springer; 2013.
- [2] H.S. Jensen. Hydrogen Sulfide Induced Concrete Corrosion of Sewer Networks [PhD Thesis]: Aalborg University; 2009.
- [3] E. Vincke, E. Van Wansele, J. Monteny, A. Beeldens, N. De Belie, L. Taerwe, et al., Influence of Polymer Addition on Biogenic Sulfuric Acid Attack of Concrete, *International Biodeterioration & Biodegradation* 49 (4) (2002) 283 – 292.
- [4] B. Singh, G. Ishwarya, M. Gupta, S.K. Bhattacharyya, *Geopolymer Concrete: A Review Of Some Recent Developments, Construction and Building Materials* 85 (2015) 78–90.
- [5] T. Bakharev, Resistance of Geopolymer Materials to Acid Attack, *Cement and Concrete Research* 35 (4) (2005) 658–670.
- [6] J. Davidovits. *Geopolymer chemistry and applications*: Geopolymer Institute.; 2008.
- [7] A. Bielefeldt, M.G.D. Gutierrez-Padilla, S. Ovtchinnikov, J. Silverstein, M. Hernandez, Bacterial Kinetics of Sulfur Oxidizing Bacteria and Their Biodeterioration Rates of Concrete Sewer Pipe Samples, *Journal of Environmental Engineering* 136 (7) (2010) 731-738.
- [8] N. De Belie, J. Monteny, A. Beeldens, E. Vincke, D. Van Gemert, W. Verstraete, Experimental Research and Prediction of the Effect of Chemical and Biogenic Sulfuric Acid on Different Types of Commercially Produced Concrete Sewer Pipes, *Cement and Concrete Research* 34 (12) (2004) 2223–2236.
- [9] N.I. Fattuhi, B.P. Hughes, The performance of cement paste and concrete subjected to sulphuric acid attack, *Cement and Concrete Research* 18 (4) (1988) 545-553.
- [10] C. Grengg, F. Mittermayr, A. Baldermann, M.E. Böttcher, A. Leis, G. Koraimann, et al., Microbiologically Induced Concrete Corrosion: A Case Study from a Combined Sewer Network, *Cement and Concrete Research* 77 (2015) 16–25.
- [11] M.G.D. Gutierrez-Padilla. Activity of Sulfur Oxidizing Microorganisms and Impacts on Concrete Pipe Corrosion [PhD thesis]: University of Colorado; 2007.
- [12] M.G.D. Gutiérrez-Padilla, A. Bielefeldt, S. Ovtchinnikov, M. Hernandez, J. Silverstein, Biogenic Sulfuric Acid Attack on Different Types of Commercially Produced Concrete Sewer Pipes, *Cement and Concrete Research* 40 (2) (2010) 293-301.
- [13] J. Herisson, E. Van Hullebusch, M. Moletta-Denat, P. Taquet, T. Chaussadent, Toward an Accelerated Biodeterioration Test to Understand the Behavior of Portland and Calcium Aluminate Cementitious Materials in Sewer Networks, *International Biodeterioration & Biodegradation* 84 (2013) 236-243.
- [14] R.L. Islander, J.S. Deviny, F. Mansfeld, A. Postyn, H. Shih, Microbial Ecology Of Crown Corrosion In Sewers, *Journal of Environmental Engineering, ASCE* 117 (6) (1991) 751–770.
- [15] J. Monteny, E. Vincke, A. Beeldens, N. De Belie, L. Taerwe, D. Van Gemert, et al., Chemical, Microbiological, and In Situ test Methods for Biogenic Sulfuric Acid Corrosion of Concrete, *Cement and Concrete Research* 30 (4) (2000) 623-634.
- [16] T. Mori, T. Nonaka, K. Tazaki, M. Koga, Y. Hikosaka, S. Noda, Interactions of Nutrients, Moisture and pH on Microbial Corrosion of Concrete Sewer Pipes, *Water Research* 26 (1) (1992) 29-37.
- [17] A. Allahverdi, F. Škvára, Sulfuric Acid Attack On Hardened Paste Of Geopolymer Cements Part 1. Mechanism of Corrosion at Relatively High Concentrations, *Ceramics Silikaty* 49 (4) (2005) 225-229.
- [18] M. Albitar, M.S. Mohamed Ali, P. Visintin, M. Drechsler, Durability evaluation of geopolymer and conventional concretes, *Construction and Building Materials* 136 (2017) 374-385.
- [19] N.K. Lee, H.K. Lee, Influence of the slag content on the chloride and sulfuric acid resistances of alkali-activated fly ash/slag paste, *Cement and Concrete Composites* 72 (2016) 168-179.
- [20] R.R. Lloyd, J.L. Provis, J.S.J. van Deventer, Acid resistance of inorganic polymer binders. 1. Corrosion rate, *Materials and Structures* 45 (1) (2012) 1-14.
- [21] A. Noushini, M. Babae, A. Castel, Suitability of heat-cured low-calcium fly ash-based geopolymer concrete for precast applications, *Magazine of Concrete Research* 68 (4) (2015) 163-177.
- [22] D.K.B. Thistlethwayte. The control of sulphides in sewerage systems. Sydney, Australia: Butterworths Pty Ltd; 1972.
- [23] J. Herisson, M. Guéguen-Minerbe, E.D. van Hullebusch, T. Chaussadent, Behaviour of different cementitious material formulations in sewer networks, *Water Science and Technology* 69 (7) (2014) 1502-1508.



- [24] M.W. Kiliswa. Composition and microstructure of concrete mixtures subjected to biogenic acid corrosion and their role in corrosion prediction of concrete outfall sewers: University of Cape Town; 2016
- [25] M.W. House, W.J. Weiss. Review of Microbially Induced Corrosion and Comments on Needs Related to Testing Procedures. Purdue University, West Lafayette, IN, USA 2014.
- [26] J.M. Pluym-Berkhout, J. Mijnsbergen, R.B. Polder, Riolerings (II), biogene zwavelzuuraantasting, *Cement* 9 (1989) 16-20.
- [27] M. Heikal, M.M. Radwan, O.K. Al-Duaij, Physico-mechanical characteristics and durability of calcium aluminate blended cement subject to different aggressive media, *Construction and Building Materials* 78 (2015) 379-385.
- [28] T. Haile, G. Nakhla, E. Allouche, Evaluation of the resistance of mortars coated with silver bearing zeolite to bacterial-induced corrosion, *Corrosion Science* 50 (3) (2008) 713-720.
- [29] X.J. Song, M. Marosszeky, M. Brungs, R. Munn. Durability of fly ash based Geopolymer concrete against sulphuric acid attack. Lyon, France 2005.
- [30] F. Rendell, R. Jauberthie, The Deterioration of Mortar in Sulphate Environments, *Construction and Building Materials* 13 (6) (1999) 321-327.
- [31] M.S.H. Khan, A. Castel, A. Akbarnezhada, S.J. Foster, M. Smith, Utilisation of steel furnace slag coarse aggregate in a low calcium fly ash geopolymer concrete, *Cement and Concrete Research* 89 (2016) 220-229.
- [32] M.S.H. Khan, A. Castel, A. Noushini, Carbonation of a low-calcium fly ash geopolymer concrete, *Magazine of Concrete Research* 69 (1) (2017) 24-34.
- [33] D.W. Law, A.A. Adam, T.K. Molyneaux, I. Patnaikuni, A. Wardhono, Long term durability properties of class F fly ash geopolymer concrete, *Materials and Structures* 48 (3) (2015) 721-731.
- [34] A. Noushini. Durability of Geopolymer Concrete in Marine Environment. Sydney, Australia: UNSW; 2018.
- [35] C.M. George. Durability of CAC concrete: Understanding the evidence. In: Scrivener KL, Young JF, editors. Mechanisms of chemical degradation of cement-based systems. London 1997.
- [36] S.K. Roy, K.B. Poh, D.O. Northwood, Durability of concrete-accelerated carbonation and weathering studies, *Building and Environment* 34 (5) (1999) 597-606.
- [37] D.O. McPolin, P.A. Basheer, A.E. Long, K.T. Grattan, T. Sun, New Test Method to Obtain pH Profiles due to Carbonation of Concretes Containing Supplementary Cementitious Materials, *Journal of Materials in Civil Engineering* 19 (11) (2007) 936-946
- [38] D.O. McPolin, P.A. Basheer, A.E. Long, Carbonation and pH in Mortars Manufactured with Supplementary Cementitious Materials, *Journal of Materials in Civil Engineering* 21 (5) (2009) 217-225.
- [39] T. Desbois, R.L. Roy, A. Pavoine, G. Platret, A. Feraille, A. Alaoui, Effect of gypsum content on sulfoaluminate mortars stability, *European Journal of Environmental and Civil Engineering* 14 (5) (2010) 579-597.
- [40] C.W. Hargis, A. Telesca, P.J.M. Monteiro, Calcium sulfoaluminate (Ye'elimite) hydration in the presence of gypsum, calcite, and vaterite, *Cement and Concrete Research* 65 (2014) 15-20.
- [41] J.L. Davis, D. Nica, K. Shields, D.J. Roberts, Analysis of concrete from corroded sewer pipe, *International Biodeterioration & Biodegradation* 42 (1) (1998) 75-84.
- [42] K.L. Scrivener, J.L. Cabiron, R. Letourneux, High-performance concretes from calcium aluminate cements, *Cement and Concrete Research* 29 (8) (1999) 1215-1223.
- [43] S. Lamberet, D. Guinot, E. Lempereur, J. Talley, C. Alt. Field investigations of high performance calcium aluminate mortar for wastewater applications. Avignon, France: IHS BRE Press; 2008.
- [44] D.J. Roberts, D. Nica, G. Zuo, J.L. Davis, Quantifying Microbially Induced Deterioration of Concrete: Initial Studies, *International Biodeterioration and Biodegradation* 49 (4) (2002) 227-234.
- [45] A.P. Joseph, J. Keller, H. Bustamante, P.L. Bond, Surface Neutralization and H<sub>2</sub>S Oxidation at Early Stages of Sewer Corrosion: Influence of Temperature, Relative Humidity and H<sub>2</sub>S Concentration, *Water Research* 46 (2012) 4235-4245.
- [46] Wells, T., Melchers, R.E., Joseph, A., Bond, P., Vitanage, D., Bustamante, H., De Grazia, J., Kuen, T., Nazimek, J., and Evans, T., A collaborative investigation of microbial corrosion of concrete sewer pipe in Australia, *Environmental Science*, 2012, 8 pp.